

Lieb-Robinson bound for constrained many-body localization

Chun Chen,^{1,*} Xiaoqun Wang,^{2,3,4,†} and Yan Chen^{5,6,‡}

¹*Max-Planck-Institut für Physik komplexer Systeme, Nöthnitzer Straße 38, 01187 Dresden, Germany*

²*Key Laboratory of Artificial Structures and Quantum Control of MOE, Shenyang National Laboratory for Materials Science, Shenyang 110016, China*

³*School of Physics and Astronomy, Tsung-Dao Lee Institute, Shanghai Jiao Tong University, Shanghai 200240, China*

⁴*Beijing Computational Science Research Center, Beijing 100084, China*

⁵*Department of Physics and State Key Laboratory of Surface Physics, Fudan University, Shanghai 200433, China*

⁶*Collaborative Innovation Center of Advanced Microstructures, Nanjing University, Nanjing 210093, China*

(Dated: May 3, 2022)

Study how quantum information propagates through the spacetime manifold may provide a useful means of identifying, distinguishing, and classifying the unconventional phases of matter fertilized by many-body effects in strongly interacting systems in and out of equilibrium. Via a fuller characterization of the key aspects regarding the novel dynamic behaviours of information, we performed such an analysis on the constrained many-body-localized phase—a newly proposed fully localized state under the infinite-interaction limit—in the quasirandom Rydberg blockade spin chain models using the thermal out-of-time-ordered commutators (OTOCs). The calculated OTOC light cone contours predict a new and hitherto unknown Lieb-Robinson bound for the constrained many-body localization, which is qualitatively different from that of the more familiar unconstrained many-body Anderson insulators normally stabilized only at the weak-interaction limit. Our corroborated numerical and analytical investigation hence suggests that the constrained many-body localization is a distinct dynamical phase of matter in constrained quantum systems whose underlying mechanism of nonergodicity is beyond the phenomenology of quasilocal integrals of motion. Further, it also consolidates the hierarchy of unconventional quantum dynamics that encompasses constrained, unconstrained, and diagonal many-body-localized regimes.

INTRODUCTION

Anderson localization (AL) describes the absence of diffusion due to strong disorders [1]. Within the last decade, physicists gradually reach a consensus that in one dimension (1D), the extended version of this essentially noninteracting phenomenon survives, provided that the added interparticle interactions are small [2–4]. This predominant viewpoint may be schematized by Fig. 1 where the inclusion of the finite interaction engenders the unconstrained many-body Anderson localization (uMBL) in the vicinity of the noninteracting point of a strongly disordered chain model.

When crafting the uMBL theoretical framework, an enduring impetus stems from the following quest: what are the fundamental differences between uMBL and its celebrated counterpart (or close relative), the AL? Indeed, if adopting a traditional perspective, these phases may look pretty similar: (i) they both exhibit insulating behaviours with exactly vanishing dc conductivities at finite temperatures for the particle and energy transports. Moreover, (ii) the level-spacing statistics based on their respective eigenspectra also fulfil the identical Poissonian distribution, suggesting the robust emergent integrability that wildly violates the ergodicity. It is therefore a milestone (iii) when the logarithmic entanglement growth was discovered in uMBL, which markedly contrasts to the rapid saturation and the sheer absence of the entanglement dynam-

ics in AL [5]. Soon afterwards, (iv) such dynamical distinctions between uMBL and AL were magnified and further resolved through the peculiar OTOC structures of uMBL and the nontriviality of its associated Lieb-Robinson (LR) bound, whereas for AL, it is consistently found that the quantum information propagation therein is completely halted [6, 7]. Remarkably, all the above-listed four hallmarks, which comprise a minimal assembly of the universal properties that defines the randomness-induced uMBL phase, can be well interpreted if a full set of local integrals of motion (LIOMs) is assumed [8, 9]. This, however, should be compared to the uMBL-like dynamics reported in several uniform and disorder-free systems [10–13] where the Poisson statistics, the zero dc conductivities, and the LIOM phenomenology may rarely be achievable.

It might be an interesting observation that since Anderson’s seminal 1958 paper on localization [1], during the last half century, most research efforts have been devoted to either the single-particle localization or the stability of its many-body generalization, especially, for the recent 15 years [2, 3]. In view of the mounting relevance of localization to the future quantum technology as well as to the theory of quantum statistical physics, could there be other fully localized phases and mechanisms that are neither AL nor uMBL?

Largely inspired by the recent breakthrough in Rydberg experiments [14], this central question was first attempted in Ref. [15] via linking it to the circumstances where the many-body interactions are not weak, but rather infinitely strong (see Fig. 1). Specifically, the first author and collaborators introduced quench disorder into the Rydberg spin chain model [15], where, inside the blockade regime, two nearest-neighbouring Rydberg atoms cannot be simultaneously excited, hence restricting the system’s evolution onto a con-

* Corresponding author.
chun6@pks.mpg.de

† Corresponding author.
xiaoqunwang@sjtu.edu.cn

‡ Corresponding author.
yanchen99@fudan.edu.cn

strained Hilbert-space manifold, which is subsequently modeled by a projection action of an infinite strength [14]. Particularly, we wondered about if localization would still persist in these strongly interacting setups when the disorder terms are maximally conflicting with the infinite interparticle interaction exemplified by the pronounced nontrivial outcomes of their mutual commutators. Nonetheless, despite a tentative tendency towards the localization, owing to the small system-size flow seen in the exact diagonalization study and the proximity to the nearby criticality, the significant finite-size fluctuations combined with the Griffiths effect render it unclear whether a genuine localization or an intermediate critical regime would eventually be reached, thus hindering a direct investigation on this topic.

To mitigate the issue, in a second paper [16] of this series we substitute the quasiperiodic modulation for the quench disorder to bypass the Griffiths region when randomizing the Rydberg array and successfully show for the first time that the envisaged robust localization can truly be stabilized even when the particle-particle interaction is simultaneously infinite in strength and transverse in direction to the randomness orientation. Crucially, we find that the resultant localization, termed constrained many-body-localized (cMBL) phase, is no longer a many-body Anderson insulator.

Concretely, by performing the static and spectral analyses, we first prove theoretically the full localization via demonstrating (1) the Poisson level statistics and (2) the strictly zero dc energy conductivity (though not explicitly shown) for the cMBL phase. Next, following the same spirit of the AL-uMBL classification, the decisive step forwarded by [16] concerns the numerical detection of the qualitatively different dynamical behaviours between cMBL and uMBL. Notably, (3) contrary to the ubiquitous single-logarithmic entanglement build-up in canonical uMBL, the half-chain von Neumann entanglement entropy in cMBL appears to grow double-logarithmically over time. Finally, (4) after parsing in detail the spatial distribution of the energy transport, a confined core structure is identified in the integral of motion (IOM) of cMBL where the appreciable nonlocal correlations dominate. These unusual characters [(3) and (4)], which have never been seen before, potentially cast doubt on the appropriateness of the LIOM phenomenology in accounting for the cMBL phase. We therefore report a new fully localized phase in [16] that features fundamental distinctions from both uMBL and AL.

A closer inspection of cMBL, however, leaves an unresolved impression that on the one hand, the unusual double-logarithmic entanglement growth manifests an ultraslow dynamical characteristic of cMBL. While, on the other hand, the considerable confined nonlocal effect embedded in the IOMs of cMBL points towards the opposite tendency of a probably faster scrambling. How can these two seemingly conflicting properties be unified in one single cMBL phase?

More importantly, what kind of trait could be the built-in genesis that distinguishes cMBL? It is known that albeit slowly, for generic MBL systems, the propagation of quantum information is strictly unbounded [5]. Instead, the primary limitation on the efficiency of information transmission is governed by the LR bounds [17], which, serving approx-

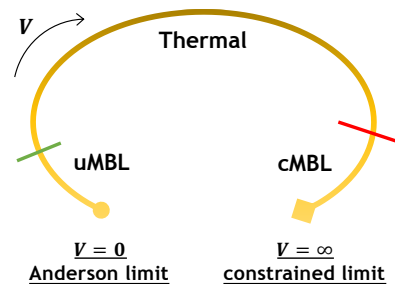


FIG. 1. The axis showing the interaction strength V for a generic randomized chain model. Anderson localization is realized at $V = 0$, whose many-body descendant, i.e., unconstrained MBL, resides right in its nearby neighbourhood of small V . By contrast, the constrained MBL is conjectured to sit around the opposite infinite- V boundary of the axis.

imately as the effective “speed of light” for nonrelativistic quantum dynamics, quantify the system’s locality and causality structures through monitoring the noncommutativity between two disjoint operators under the unitary time evolution. In the absence of constraints, this kind of information flow gives rise to a characteristic logarithmic light cone that designates the territory of the uMBL phase. Then, what does the light cone contour of the newly found cMBL look like? What is its associated LR bound, and how does it shape the cMBL’s light cone front?

It turns out that the crux of these questions lies in the dynamics of quantum information, i.e., the spatiotemporal information spreading pattern. One proper tool capable of capturing such a spacetime complexity beyond the autocorrelation function is the OTOC, originally proposed by Larkin and Ovchinnikov in semiclassical theory of superconductivity [18] and popularized recently by Kitaev in quantum chaos and quantum thermalization [19],

$$C_{\beta}^{AB}(i, j; t, t') = \langle [A(i, t), B(j, t')]^{\dagger} [A(i, t), B(j, t')] \rangle_{\beta}, \quad (1)$$

where A, B are the specified Heisenberg operators, e.g., $A(i, t) := e^{iHt} A(i, 0) e^{-iHt}$. See also the Methods section for additional derivations on this definition. In present work, we will exclusively focus on the thermal ensemble average of such a quantity at infinite temperature, i.e., $\beta = 0$, and keep setting $\hbar = 1$.

Let us briefly outline the employed tactic. The central object we scrutinize is OTOC, which amounts to the Frobenius norm of the commutator squared, thereby linking directly to the LR bound. Furthermore, by compiling the time evolution of OTOC at fine distances between A and B , one can visualize the spatiotemporal arrangement of the light cone to decode the content on how the information is processed. Previous studies [7] have demonstrated that this OTOC light cone front is dictated by the LR bound. Hence, OTOC comprises a useful device to bridge the respective propagations of quantum information along space and time under the guiding principles of locality and quantum mechanics. Put differently, via computing the OTOC light cone, one can deduce the detailed form of the LR bound, the gained knowledge of which in turn facili-

tates the deciphering of the complicated OTOC structures.

Although OTOC and LR bound might seem auxiliary to the development of uMBL, they assume here a vital role in elucidating the more subtle underpinnings of the unconventional localization in constrained quantum settings. Being a joint spacetime identity, they are bound to yield more comprehensive information about the underlying quantum dynamics than the time-dependent half-chain entanglement entropy. For instance, as we will show below, a descendent entropy bound compatible with the observed double-logarithmic entanglement growth [16] can be derived from the cMBL's LR bound via the so-called OTOC-Rényi-entropy theorem [6, 20].

RESULTS

Model

The quasirandom Rydberg chain model may be describable by the following simple Hamiltonian [15, 16],

$$H_{\text{qp}} = \sum_i \left[g_i \tilde{X}_i + h_i \tilde{Z}_i \right], \quad (2)$$

where the coefficients assume

$$g_i = g_x + W_x \cos \left[\frac{2\pi i}{\phi} + \phi_x \right], \quad (3)$$

$$h_i = W_z \cos \left[\frac{2\pi i}{\phi} + \phi_z \right], \quad (4)$$

and $\tilde{X}_i := P\sigma_i^x P$, $\tilde{Z}_i := P\sigma_i^z P$ denote the projected Pauli matrices under the action of a global projector

$$P := \prod_i \left[(3 + \sigma_i^z + \sigma_{i+1}^z - \sigma_i^z \sigma_{i+1}^z) / 4 \right], \quad (5)$$

which annihilates motifs of $\downarrow\downarrow$ -configuration over any adjacent sites of the chain. The quasiperiodic modulation is then controlled by the inverse golden ratio $1/\phi = (\sqrt{5} - 1)/2$ and $\phi_x, \phi_z \in [-\pi, \pi)$ are the independent random overall phase shifts. The real Hamiltonian (2) is manifestly invariant under time reversal $\mathbb{T} := K$, i.e., the complex conjugation and once $W_z = 0$, it additionally anticommutes with the particle-hole transformation $P := \prod_i \sigma_i^z$. Throughout this paper, we will choose $W_x = 1$ to be the energy scale, viz., the chain is quasirandom at least along the x direction. Since the exact-diagonalization calculations below have always been sampled over more than 10^3 quasiperiodic realizations, to ease the notation, we also tacitly assume that all the physical quantities pertinent to this work are quasirandom averages over an adequate amount of distributions. See the Methods section for more explanations on the numerical procedures.

The hard-core boson representation

To some degree, discussions in this subsection duplicate certain material of [16]. However, we deem it advisable to preserve this parallelism and continue on unpacking our theoretical model through this and next subsections so that sufficient background and hidden motivation might become more transparent.

To unravel the interplay between the finite tunable randomness and the infinite interparticle interaction as encapsulated in model (2), we introduce the hard-core boson operators b_i^\dagger, b_i at each site i to describe the local pseudospin-1/2 subsystem that mimics the lattice gas of Rydberg atoms with the ground state $|g\rangle_i = |\uparrow\rangle_i$ and the Rydberg excitation state $|r\rangle_i = |\downarrow\rangle_i$. In terms of these hard-core bosons, the Pauli spin matrices can be rearranged as follows,

$$b_i^\dagger + b_i = |r\rangle_i \langle g| + |g\rangle_i \langle r| = |\downarrow\rangle_i \langle \uparrow| + |\uparrow\rangle_i \langle \downarrow| = \sigma_i^x, \quad (6)$$

$$b_i^\dagger b_i = n_i = |r\rangle_i \langle r| = |\downarrow\rangle_i \langle \downarrow| = \frac{(1 - \sigma_i^z)}{2}, \quad (7)$$

where $n_i = 0, 1$ is the local boson occupation number. Equipped with the above expressions, the Hamiltonian (2) can alternatively be mapped onto an array of neutral atoms loaded in the Rydberg blockade regime,

$$H_{\text{qp}} = H_x + H_z + H_V, \quad (8)$$

$$H_x = \sum_i g_i (b_i^\dagger + b_i), \quad (9)$$

$$H_z = \sum_i h_i (1 - 2n_i), \quad (10)$$

$$H_V = \sum_i V_1 n_i n_{i+1}, \quad V_1 = \infty. \quad (11)$$

Here g_i, h_i are respectively proportional to the onsite Rabi frequency and the frequency detuning. The long-range repulsive van der Waals interaction has been truncated in (11) to retain merely the nearest-neighbour interaction whose strength V_1 has been lifted to infinity, producing a blockade radius of $a < R_b < 2a$. Clearly, the system's particle-number conservation is explicitly broken by H_x , so the total energy remains the only conserved quantity of the model. Furthermore, without H_V , $H_0 = H_x + H_z$ itself is a free Hamiltonian of decoupled spins, each undergoing an independent Larmor precession about their local random fields.

Consequently, the constrained Rydberg atomic chain under scrutiny simply consists of two constituents: a randomized but noninteracting term H_0 and a nearest-neighbour density-density interacting term H_V featured by an infinite repulsion.

Such a compact form with the presence of a single ‘‘spin-like’’ sector as well as the reduction of the ‘‘effective’’ onsite Hilbert-space dimension from the usual value of 2 in normal spin chain to the current smaller number of the golden ratio $\phi = 1.618\dots$ (in the sense that at larger lengths L , the total Hilbert-space dimension of the constrained Rydberg chain increases as per a function of ϕ^L) prompt us to regard the minimal model (8) as the fundamental building block for investigating the more generic quantum systems with constraints, like the t - J type Hamiltonians that model the 1D cuprate compounds.

More precisely, in light of the following nonequivalent commutation relations,

$$[H_x, H_V] \neq 0, \quad (12)$$

$$[H_z, H_V] = 0, \quad (13)$$

the constrained Hamiltonian (8) is expected to accommodate two distinct physical extremes.

1. **Diagonal MBL.** When $|W_z| \gg |g_x|, |W_x|$, the chain approaches the diagonal limit where the role of the infinite interaction has been effectively minimized and the resulting diagonal MBL (dMBL) state represents a variant of the many-body Anderson insulator with possibly enhanced robustness. In Figs. 4 and 5 below, we choose the following set of parameters to numerically realize a representative localized state deeply inside the dMBL phase,

$$\text{dMBL: } g_x/W_x = 0.9 \quad \text{and} \quad W_z/W_x = 8, \quad (14)$$

whose approximate level-spacing ratio after random average has already been almost Poissonian ($[r] \approx 0.386$) at $L = 22$.

2. **Constrained MBL.** By comparison, once $|g_x|, |W_x| \gg |W_z|$, the system enters the so-called off-diagonal constrained limit—the true “infinite-interaction limit” we are after—where the mutual impacts from the modest randomness and the infinite interaction are contrastingly maximized. Particularly, their constructive interplay yields the sought infinite-interaction-triggered MBL state which is drastically different from the “infinite-randomness-controlled” uMBL customarily arising from the opposite limit of the weak interaction. The prototypical parameters we use across Figs. 2 and 3 that are situated well within the cMBL dome read,

$$\text{cMBL: } g_x/W_x = 0.9 \quad \text{and} \quad W_z/W_x = 0, \quad (15)$$

whose averaged level-statistics data shows similar convergence towards the Poisson value with $[r] \approx 0.387$ at $L = 22$. For more evidence bolstering the stabilization of the unconventional localization, please refer to [16].

Naïvely, we anticipate that no apparent duality would directly link these two extremes.

The mixed-field Ising representation

Since our main attention is focused on a single lattice Hamiltonian, it is beneficial to explain why the pursued physics from solving Eq. (2) does not suffer the nominal drawbacks of being specialized. One shortest answer to this concern can be conceived by noticing that in terms of the spin operators from (6) and (7), the Hamiltonian (8) can also be recast into a form of the strongly interacting version of the paradigmatic mixed-field Ising chain model,

$$H_{\text{qp}} = \sum_i g_i \sigma_i^x + \sum_i h_i \sigma_i^z + \sum_i \frac{V_1}{4} (1 - \sigma_i^z - \sigma_{i+1}^z + \sigma_i^z \sigma_{i+1}^z). \quad (16)$$

Considering the fact that a grand portion of the uMBL theoretical framework was developed from investigating the disordered Heisenberg *XXZ* chain as well as the instrumental

role played by its clean version in formulating the theory of quantum integrability, there is a good reason to anticipate that the current series of works targeting the different (but equally important) strongly interacting, quasirandom transverse-field Ising model in a longitudinal field embodies the essential physics towards a new dynamical universality class of the nonequilibrium eigenstate phases of matter.

For the sake of completeness, let us make a short detour to re-ponder the 1D chain model of spinless fermions subject to the randomness in either the nearest-neighbour hopping t_i or the onsite potential ε_i ,

$$H_{\text{sf}} = \sum_i (t_i \hat{c}_i^\dagger \hat{c}_{i+1} + \text{H.c.}) + \sum_i \varepsilon_i \hat{n}_i + U \sum_i \hat{n}_i \hat{n}_{i+1}, \quad (17)$$

where $\hat{c}_i^\dagger, \hat{c}_i$ are the spinless fermionic operators at site i and hatted $\hat{n}_i = \hat{c}_i^\dagger \hat{c}_i$ denotes the accompanying local fermion density. As aforementioned, H_{sf} at finite U is arguably one of the most extensively studied models in the context of uMBL, which is tantamount to the disordered Heisenberg *XXZ* chain upon a Jordan-Wigner transformation. Due to the strict fermion number conservation, when $U = 0$, the LIOM of H_{sf} at strong randomness may be expandable into a sequence of local fermion density operators that nearly commutes with the density-density interaction term. By analogy to the preceding rationale, this hints that when extrapolating $U \rightarrow \infty$, the system would presumably flow towards the dMBL limit, and roughly speaking, H_{sf} behaves like a single “charge-like” sector.

By all accounts, the specific but archetype H_{qp} and H_{sf} may be regarded as the two most fundamental minimal Hamiltonians for capturing the broad spectrum of the constrained models. Typically these spin- and charge-like sectors will intimately intertwine with each other to furnish the Hilbert space of a spinful system (note that the familiar spin-charge separation occurs only within an approximate low-energy ground-state manifold), one might thus speculate that the prospective state of localization in constrained quantum platforms may be a hybrid of the dMBL and cMBL phases. In this sense, our proposed model and the obtained results could bear the usefulness in assessing the collective influence from disorder, interaction, and constraint.

It is noteworthy that the kinetic constraint has been successfully implemented in the Rydberg blockade chain [14] and the quasiperiodic modulation has already attained a feasible status in the monumental experiments [21, 22] to achieve the signature of MBL under the unconstrained circumstances. Accordingly, besides the pure theoretical interests, the actual merit of model (2) resides right in its high experimental relevance.

LR bound in the cMBL phase

Upon the extensive preparation so far, we are now ready to declare our major analytical and numerical findings regarding the dynamics of quantum information in the randomized Rydberg blockade chains.

To proceed, we will first state an assertion on the analytical expression of the LR bound for the cMBL phase and contrast this postulate and the ensuing light cone front with the established results of the uMBL phase. Next, numerical evidence

based on the exact diagonalization calculations is supplied to verify the postulated bound formula with a demonstration on its correctness in capturing the OTOC profiles along both the space and time directions. Finally, we show that the LIOM phenomenology, despite being powerful enough to account for the uMBL's LR bound, fails in the cMBL case. As pinpointed by our previous work [16], the missing piece could stem from the thermal-like core structures embedded in the IOMs of the cMBL phase. To incorporate this key ingredient, a new phenomenological theory is put forward, which potentially catches the common thread that links the multiple intrinsic properties of the unconventional constrained localization, thereby allowing a qualitative understanding about its unusual LR bound.

Postulate.—One principal result of the present work is to propose the following new LR bound for the definition of the cMBL phase:

$$\| [A(x, t), B(0, 0)] \|_{\text{cMBL}} \lesssim c \exp[-\eta \ln |x| + \xi \ln \ln |t|], \quad (18)$$

where the positive exponents satisfy $\xi > \eta$ and $\| \cdot \|$ stands for the operator norm, i.e., the modulus of the operator's maximal singular value, which normally exceeds the operator's Frobenius norm, $\|A\|_{\text{F}} := \sqrt{\text{Tr}(A^\dagger A) / \text{Tr}(\mathbb{1})} \leq \|A\|$.

From (18), it is recognized that the development of the OTOC in cMBL is featured concurrently by a logarithmic growth over time (up to some power) and a power-law fall-off across space. Select a physical threshold ε , the cMBL's OTOC light cone front can then be captured by

$$\ln |t| \approx \left(\frac{\varepsilon}{c^2} \right)^{1/(2\xi)} \cdot |x|^{\eta/\xi}. \quad (19)$$

Being a comparison, we list below the known LR bound for the familiar uMBL phase [7, 23]:

$$\| [A(x, t), B(0, 0)] \|_{\text{uMBL}} \lesssim f \exp[-\varsigma |x| + \nu \ln |t|]. \quad (20)$$

As opposed to (19), Eq. (20) predicts that for uMBL, the rise of OTOC follows a power-law function of time; simultaneously its weight along the spatial coordinate becomes exponentially attenuated when deviating from the light cone. The resulting front in this case is given by

$$\ln |t| \approx \frac{1}{2\nu} \ln \left(\frac{\varepsilon}{f^2} \right) + \frac{\varsigma}{\nu} |x|. \quad (21)$$

Be aware of the point that this seemingly minor quantitative change in the exponent of the light cone front [from 1 in (21) to η/ξ in (19)] results nonetheless from the qualitative difference between the two distinct categories of the LR bounds in the actual contents of their respective formulae [see (18) and (20)].

Numerical verification.—Figure 2 provides numerical evidence justifying the appropriateness of this new LR bound [Eq. (18)] for cMBL. Specifically:

- (i) The power-law fit between $\log(t)$ and the operators' distance $|i-j|$ of the OTOC front [white dashed lines in

Figs. 2(a),(d)] yields an exponent $\eta/\xi < 1$ at a properly specified threshold (see below) for Eq. (19), indicating the information spreading in cMBL seems algebraically more efficient than that of uMBL where this exponent equals 1 as per (21).

- (ii) The respective horizontal cuts across the light cone images are presented through panels (b),(e) for the two chosen instants, from which a threshold of the information front can be identified at the cusp where two separate power-law fits of the OTOC data above and below this threshold intersect.
- (iii) Figures 2(c),(f) plot the characteristic logarithmic growth of OTOC where the kinks that appear when OTOC surpasses the identified threshold echo the cusps on the curves of the spatially power-law decay.

Regarding these findings, several comments are in order. First, the front shape, the spatial variation, and the temporal development of the OTOC light cone are normally interrelated because determining any two of them will naturally settle the remaining one. For instance, in view of the reasonably good fits in panels [(a),(d)] and [(c),(f)], for consistency the OTOC's spatial attenuation is then anticipated to follow a power law. Second, the estimate of the LR bound, in practice, mainly targets the region close to the light cone front, therefore, considering the finite-size fluctuations, it is possible that some elaborate choices of the threshold (like those indicated by the kinks and cusps) would be superior than other plain assignments. Third, the logarithmic temporal growth of OTOC constitutes one decisive result of the current paper. As a direct implication, the establishment of such a logarithmic rise of OTOC reinforces the prediction on the double-logarithmic entanglement build-up in cMBL. Moreover, from either the numerical or experimental viewpoint, the confirmation of such a single-log function could be considerably easier and more reliable than the detection for the cMBL's double-log entanglement growth. Finally, in addition to $[C_{\beta=0}^{ZZ}]$, the cMBL's $[C_{\beta=0}^{ZX}]$ and $[C_{\beta=0}^{XX}]$ components, as illustrated by Fig. 3, also show the qualitatively similar dynamical behaviours.

The above numerical observations thus highlight the necessity of scrutinizing the spatial and temporal profiles of the OTOC contours on an equal footing in that although for cMBL the temporal growth of OTOC (entanglement entropy) has slowed to an unusual logarithmic (double-logarithmic) function of time, its spatial leakage of quantum information has nonetheless been enhanced from an exponential suppression to a power-law decay. If take the uMBL phase as a reference state, then it turns out that for cMBL its temporal and spatial evolutions of the OTOCs have however been oppositely tipped towards localization and thermalization (with respect to uMBL). As a result, their conspiracy yields the numerically smaller exponent $\eta/\xi < 1$ for the observed light cone front. In this regard, OTOCs paint a unified spacetime picture of the information propagation and potentially hint that cMBL may be a faster information scrambler than uMBL. Despite being consistent with our prior analysis on the embedded thermal-like core inside the IOM of cMBL, this speculation on

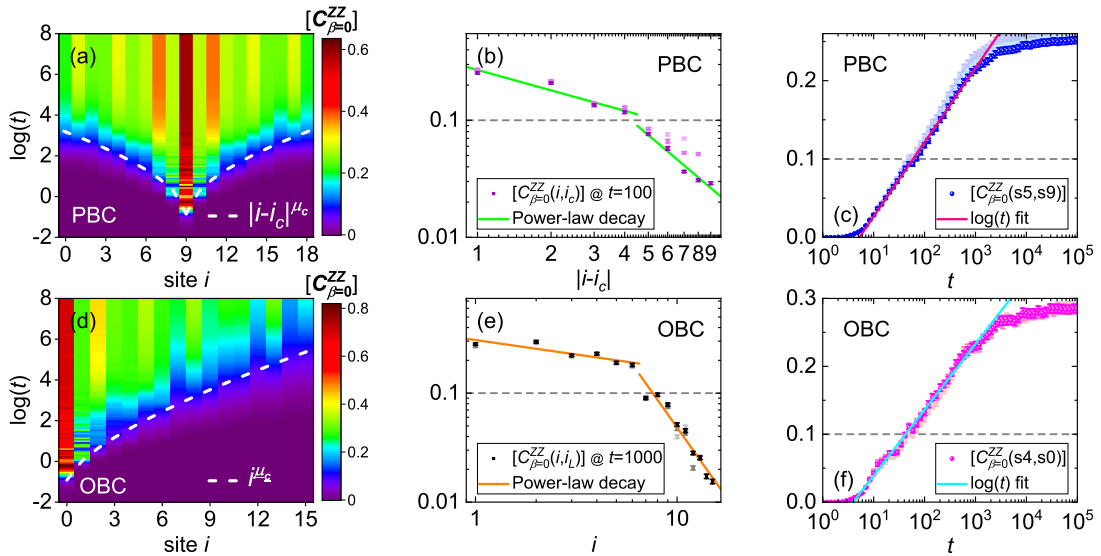


FIG. 2. The cMBL's light cones via $[C_{\beta=0}^{ZZ}]$, the ensemble-averaged OTOC. Here, the cMBL phase is ensured by selecting $g_x/W_x = 0.9$ and $W_z/W_x = 0$ [16]. The first row [(a)-(c)] targets the periodic boundary conditions (PBCs) with system size $L = 19$, while the second row [(d)-(f)] implements the same calculation with $L = 16$ under the open boundary conditions (OBCs). In images (a),(d), the white dashed lines delineate the OTOC fronts as per a power-law fit between $\log(t)$ and the operators' spacing. The obtained power-law exponent $\mu_c \approx 0.565$ [$\mu_c \approx 0.682$] is less than 1, so the information spread inside cMBL is algebraically faster than uMBL. The second column [(b),(e)] depicts the spatial extent of the front, viz., the horizontal cuts in (a),(d) along the characteristic moments, from which a unique threshold $[C_{\beta=0}^{ZZ}] \approx 0.1$ (marked by grey dashed lines) can be identified by noticing that the OTOC above and below this value follows separately two individual power laws. The third column [(c),(f)] standing for the vertical cuts in (a),(d) on specified sites illustrates the logarithmic temporal growth of OTOC at cMBL. Accompanied to the cusps of (b),(e), once OTOC exceeds the threshold, there arise the corresponding signatures of kinks in the time profiles of (c),(f). Light to solid colours in (b),(c) [(e),(f)] cover $L = 15, 17, 19$ [$L = 12, 14, 16$], respectively. Except for the contour plots, all data points shown in this work are with error bars which exhibit the standard deviations of the corresponding averaged quantities over more than 10^3 quasirandom samples. In cases where some error bars are invisible, it is because their magnitudes are smaller than the used symbol sizes. Also, all the lines overlaid are obtained from the best fits of the selected data sets by making use of the weighted least-square method.

the information scrambling does not necessarily contradict the phenomenology of full localization, because unlike the absolute disappearance of the transports for conserved quantities such as energy and particle number, it has been well appreciated that the information spreading in general MBL systems, although being significantly reduced, continues even in the thermodynamic limit and does not completely cease at all [4]. We like to remind the reader that the eigenspectral statistics of both the cMBL and dMBL phases are Poissonian such that the energy transports and the associated dc conductivities in both

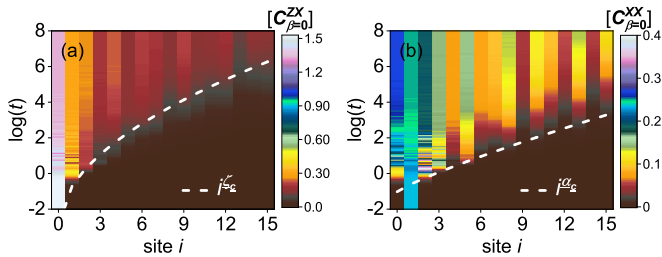


FIG. 3. The cMBL's light cones via $[C_{\beta=0}^{ZX}]$ and $[C_{\beta=0}^{XX}]$ under OBCs. The Hamiltonian parameters remain the same as in Fig. 2. Both power-law fitting exponents are less than 1 with $\zeta_c \approx 0.516$ and $\alpha_c \approx 0.849$.

regimes vanish identically. Further, through analyzing multiple kinds of entanglement variances, we also demonstrated an abrupt eigenstate transition between the cMBL and the thermal phases [16]. We hence resolve the skepticism about the compatibility between the double-logarithmic entanglement growth and the emergent pronounced nonlocal correlations over the confined length scales.

Table I sums up the dynamical features that single cMBL out as a new state of matter relative to both dMBL and uMBL, from which a phase-like hierarchy that encompasses cMBL, uMBL, and dMBL, as well as an echelon relationship among OTOC, entanglement entropy, and quantum Fisher information (QFI) can be perceived. Here, as usual, we define the von

TABLE I. Dynamics hierarchies of OTOC light cone front, entanglement entropy, and quantum Fisher information spanning constrained, unconstrained, and diagonal MBL phases.

	$\text{LCF}_{[\text{OTOC}]}$	$[S_N]$	[QFI]
cMBL	$x \sim [\log(t)]^{>1}$	$\log \log(t)$	$\log \log \log(t)$
uMBL	$x \sim [\log(t)]^1$	$\log(t)$	$\log \log(t)$
dMBL	$x \sim [\log(t)]^{<1}$	t^α	$\log(t)$

Neumann entanglement entropy upon tracing out the degrees of freedom in half of the system,

$$S_{\text{vN}}(t) := -\text{Tr}[\rho_R(t) \log_2 \rho_R(t)], \quad (22)$$

where ρ_R is the reduced density matrix of the right half chain. Likewise, via initialization from the prepared Néel state $|\psi\rangle$ at $t=0$, the QFI density acquires a simplified form analogous to the connected correlation function of the staggered spin-imbalance operator $I := (1/L) \sum_{i=1}^L (-1)^i \sigma_i^z$, i.e.,

$$f_Q(t) := 4L [\langle \psi(t) | I^2 | \psi(t) \rangle - \langle \psi(t) | I | \psi(t) \rangle^2]. \quad (23)$$

A detailed account on the time-evolving profiles of $[S_{\text{vN}}]$ and $[f_Q]$ was documented in [16]. For conciseness, we draw attention here chiefly to their temporal attributes.

Phenomenology derivation.—Before embarking on the LR bound for cMBL, it might be worthwhile to reexamine the applicability of the scenario involving the well-defined quasiloocal integrals of motion (LIOMs) [4, 8, 9]. Since the model (2) is local in projected Hilbert space, the naïve estimate of the LR bound produces a linear light cone typical for the thermal states. Within uMBL, the LIOM scenario could come to the rescue, which posits that IOMs are not only commuting but also spatially quasiloocal. Consequently, by rewriting a generic short-range disordered Hamiltonian in the IOM representation,

$$H = \sum_{Z:\{j,N\}} h_Z = \sum_{Z:\{j,N\}} \sum_n \langle n | h_Z | n \rangle | n \rangle \langle n |, \quad (24)$$

where $\{|n\rangle\}$ is the complete set of eigenstates and $\tilde{h}_Z := \sum_n \langle n | h_Z | n \rangle | n \rangle \langle n |$ is the IOM associated to the local term h_Z , one can readily derive a refined LR bound that engenders a logarithmic light cone,

$$\| [A(x, t), B(0, 0)] \|_{\text{uMBL}} \lesssim f' \frac{|t|}{e^{s|x|/\nu}}. \quad (25)$$

Here the numerator $|t|$ results from the commutativity property $[\tilde{h}_{Z'}, \tilde{h}_Z] = 0$ and the asserted quasiloquality of IOMs, viz.,

$$\sum_{Z \ni i, j} \|\tilde{h}_Z\| \leq \lambda'_0 \exp\left[-\frac{\zeta}{\nu} \text{dist}(i, j)\right], \quad (26)$$

gives rise to the exponential in the denominator. The above derivation of (25) was first reported by Refs. [6, 7, 23]. For illustration, we simply reproduce their procedures of handling the key assumptions. Nevertheless, a parallel reasoning that mirrors the uMBL case does not work for cMBL. First, the numerical light cones from Figs. 2(a),(d) clearly violate the predictions of (21) and (25). Second, Figs. 2(b),(e) suggest that for cMBL the exponential fall-off in (26) should be replaced by a power law, then a straight application of the LIOM scenario yields an LR bound even looser than that of the thermal linear light cone, contradictory to our starting assumption on localization.

Phenomenologically, Ref. [16] reveals a nonnegligible thermal core enclosed by the IOM of cMBL, which naturally induces a length scale χ separating the differing short-range and

long-range physics. Furthermore, this confined nonlocality, as demonstrated below, assumes an active role in deriving the cMBL's LR bound, and thereby hints at the necessity to partially abandon the LIOM framework. The basic idea instead is to reformulate a Hastings-Koma (HK) series suitable for MBL by switching from the Heisenberg picture to the interaction picture where χ acquires a dynamical character.

To analytically address Eqs. (18) and (19), we adopt the strategies of Refs. [24, 25] and upgrade the original scheme from the few-body interactions in an ergodic system to the more general k -body interactions in the MBL setting.

A full derivation that leads to the Eq. (30) below has been detailed in [26]. For conciseness, we summarize here the major constituents involved in the following three successive steps. Concretely, we first divide the Hamiltonian (2) into the short-range [$\text{diam}(Z^{sr}) \leq \chi$] and the long-range [$\text{diam}(Z^{lr}) > \chi$] parts,

$$H_{\text{qp}} = H^{sr} + H^{lr} = \sum_{Z^{sr}} \tilde{h}_{Z^{sr}} + \sum_{Z^{lr}} \tilde{h}_{Z^{lr}}, \quad (27)$$

according to which the interaction-picture operator reads $A_I(t) := e^{iH^{sr}t} A e^{-iH^{sr}t}$. The necessary connection between the Heisenberg and the interaction pictures is via the unitary scattering matrix, $A(t) = \mathcal{S}^\dagger(t) A_I(t) \mathcal{S}(t)$, $\mathcal{S}(t) = e^{iH^{sr}t} e^{-iHt}$, as usual.

Next, the short-range contribution to the LR bound arising from the thermal core can be estimated by using the standard HK series,

$$\frac{\| [A_I(t), B] \|}{\| A \| \| B \|} \leq s |X| \exp[v|t| - \text{dist}(X, Y)/\chi(t)], \quad (28)$$

which indicates that the long-range operator $A_I(t)$ may be approximated by a sequence of intermediate operators whose supports are strictly finite-ranged,

$$\| A_I(\ell, t) - A_I(t) \| \leq s \| A \| |X| \exp(-\ell), \quad (29)$$

where $A_I(\ell, t) := e^{iH_\Lambda^{sr}t} \left\{ \int_{\mathbb{B}} d\mu(U) U A U^\dagger \right\} e^{-iH_\Lambda^{sr}t}$ [27] and \mathbb{B} denotes the complement to the ball $\mathbb{B} := \{i \in \Lambda_s | \text{dist}(i, X) \leq R_\ell(t)\}$ whose radius $R_\ell(t) = R(t) + \ell\chi = \chi v|t| + \ell\chi$, $\ell = 0, 1, 2, \dots$. Here, X, Y represent the lattice sets holding the operators A, B , respectively.

Finally, the incorporation of the contributions from H^{lr} entails the extension of the HK's scheme for the explicit inclusion of the overlapping conditions between the two disjoint intermediate operators, which bear the crucial $|t|$ -dependence. Then, by invoking the discrete convolution amid the reduction of the augmented HK series, one obtains the following LR bound for the generic k -body Hamiltonian featuring the power-law decaying strengths,

$$\frac{\| [A(t), B] \|}{\| A \| \| B \|} \leq s |X| (1 + e) \left\{ \frac{2e}{e-1} e^{vt - \text{dist}(X, Y)/\chi(t)} + w^{-\eta} \cdot \frac{\exp\{g' \chi^{D-\eta} [R(t)]^D t\}}{[\text{dist}(X, Y)/R(t)]^\eta} \right\}, \quad (30)$$

where D is the spatial dimension, $|X|$ is the cardinality of set X , and s, v, w, g' are positive coefficients. Up to prefactors,

Eq. (30) resembles the result of Ref. [25]—the essential improvement relative to the HK’s bound [24] resides in the renormalization of the various contents under the influence of the emergent dynamical length scale. From a broad perspective, Eq. (30) also illustrates the probable suitability of extending the generalized HK’s methods to the wide realm of MBL.

The derivation so far is somewhat quasi-rigorous except that it is based on certain fundamental assumptions that are of the phenomenological nature. For example, both the form as well as the coefficients employed to describe the spatial distribution of the IOM’s weights [like Eq. (26)] are hypothesized because without exactly solving the model, they cannot be fully justified or expressed analytically in terms of the microscopic parameters of the investigated lattice Hamiltonian. To make progress, usually one has to rely on the physical insights gained from the finite-size numerics. The validity of the overall procedure can then be crosschecked by consistency.

In the case at hand, we do find such a solution for the phenomenological quantity χ as a function of time so that the simulated light cone structures of the OTOCs could be qualitatively comprehended to some extent. Indeed, specialized to cMBL, one finds that for $2D - 1 < \eta < 2D$, by devising

$$\chi(t) = \rho(\ln t)^{at^b} \quad (31)$$

and substituting

$$a = -\frac{b}{D+1} = \frac{1}{2D-\eta} > 1, \quad (32)$$

$$\rho = \left[\frac{1}{v^D g'} \frac{\eta(\eta - D + 1)}{2D - \eta} \right]^{\frac{1}{2D-\eta}}, \quad (33)$$

the LR bound in Eq. (30) simplifies to a desired form,

$$\frac{\| [A(t), B] \|}{\| A \| \| B \|} \leq s |X| (1 + e) \left\{ \frac{2e}{e-1} \exp \left[vt - \frac{\text{dist}(X, Y)}{\rho(\ln t)^{at^b}} \right] + \left(\frac{v\rho}{w} \right)^\eta \cdot \frac{(\ln t)^{a\eta}}{[\text{dist}(X, Y)]^\eta} \right\}. \quad (34)$$

Specifically, Eq. (34) demonstrates that the OTOC of A, B is bounded by the line $\text{dist}(X, Y) \propto (\ln t)^{a'}$ with $a' > a > 1$, because for arbitrary threshold ε , there exists a critical moment $t_c < \infty$ such that whenever $\text{dist}(X, Y) \gtrsim (\ln t)^{a'}$, $\| [A(t_c), B] \| < \varepsilon$. This rephrases asymptotically the relation (19) of our numerical observations on cMBL. Meanwhile, the implication regarding the shrinkage of $\chi(t)$ is not only compatible with the general requisite for localization, but it also signals the potential stability of the cMBL phase under the thermodynamic limit—a confined thermal core has zero measure when the space-time coordinates approach infinity.

To summarize, the overall rationale behind the above derivation is that by imposing the condition that the analytical formula (30) explains the numerical OTOC light cones, a physical solution for the dynamical length scale can be obtained as (31), which completes the main thread of the developed theory and renders the definition of the cMBL phase being self-consistent.

The entropy bound

This cMBL bound, together with the OTOC-Rényi-entropy theorem [6, 20], yields a bound for the rise of the bipartite entropy on a finite open chain starting from the randomized product states,

$$[S_R^{(2)}(t)] \lesssim -\ln(\vartheta - \varrho \ln t), \quad (35)$$

where ϑ, ϱ are nonuniversal t -independent constants and $\vartheta > \varrho \ln t$ sets the saturation time scale, i.e., $t < t_{\text{sat}}$. Then, via the elementary inequalities, it is straightforwardly proven that $\ln \ln(te^{\vartheta/\varrho}) + \ln(\varrho/\vartheta^2) \leq -\ln(\vartheta - \varrho \ln t)$, implying that the observed double-logarithmic entanglement build-up in cMBL [16] fulfills this entropy bound.

LR bound in the dMBL phase

One central message of Ref. [16] concerns the eigenstate transition between cMBL and dMBL under the increase of W_z . Thrived upon that prediction, Fig. 4 illustrates that the OTOC light cone of dMBL differs in fundamental aspects from that of cMBL.

- (i) The power-law fit between $\log(t)$ and the operator distance of the OTOC front [white dashed lines in Figs. 4(a),(d)] delivers an exponent greater than 1, suggesting the information transmission through dMBL is algebraically less efficient than that of uMBL.
- (ii) The horizontal cuts of the light cone images are displayed by (b),(e) for two representative moments, from which it can be observed that to dMBL, the OTOC’s spatial decay is delineated by a stretched exponential function, reflecting the fact that dMBL is a more robust localization phase, consistent with the anticipation that constraints generally stymie certain intermediate channels of relaxation.
- (iii) In line with uMBL, the temporal growth of OTOC in dMBL obeys a usual power-law function of time, as is seen from Figs. 4(c),(f).

For completeness, qualitatively analogous results on the OTOC contours for the dMBL’s $[C_{\beta=0}^{ZX}]$ and $[C_{\beta=0}^{ZZ}]$ components are supplied by Fig. 5. Because IOMs of dMBL are dressed local \tilde{Z}_i -operators [15, 16], the saturated values of $[C_{\beta=0}^{ZZ}]$ there turn out to be significantly smaller than $[C_{\beta=0}^{XX}]$ [7]. However, no such discrepancy arises in cMBL.

Conceptually, the dMBL phase is described by the LIOM phenomenology [15, 16]. Particularly, the above OTOC results can be comprehended to a large extent by introducing the following LR bound for dMBL,

$$\| [A(x, t), B(0, 0)] \|_{\text{dMBL}} \lesssim \tilde{f} \exp \left[-\tilde{\zeta} |x|^{\tilde{\kappa}} + \tilde{\nu} \ln |t| \right]. \quad (36)$$

The derivation of (36) mirrors that for (25). Compared to the uMBL case, the essential difference lies at the functional change of the spatial weight from the canonical exponential decay in uMBL to the more severe stretched exponential fall-off in dMBL, as can be inferred from the condition that the exponent $\tilde{\kappa} > 1$. Therefore, after a minor modification of (26)

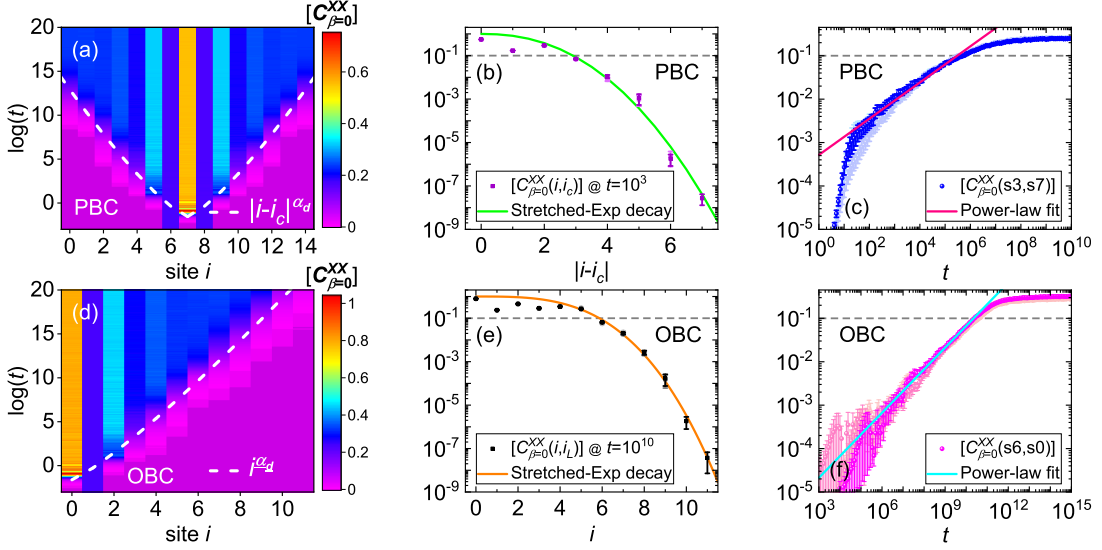


FIG. 4. The dMBL's light cones via $[C_{\beta=0}^{XX}]$. Here, the dMBL phase is stabilized by choosing $g_x/W_x = 0.9$ and $W_z/W_x = 8$ [16]. [(a)-(c)] target PBCs with system size $L = 15$; [(d)-(f)] execute the same calculation with $L = 12$ utilizing OBCs. In (a),(d), the white dashed lines delimit the OTOC fronts (determined from the same threshold $[C_{\beta=0}^{XX}] \approx 0.1$) as per a power-law fit between $\log(t)$ and the operator separation. The obtained power-law exponent $\alpha_d \approx 1.289$ ($\alpha_d \approx 1.184$) is greater than 1, so the information spread in dMBL is algebraically slower than that of uMBL. [(b),(e)] depict the spatial variation of the light cone along the horizontal cuts in (a),(d). The spatial attenuation of the OTOC at dMBL is fitted by a stretched exponential. [(c),(f)] present the vertical cuts in (a),(d) at specified sites to exhibit the power-law temporal growth of OTOC inside dMBL. Light to solid colours of (b),(c) [(e),(f)] correspond to $L = 11, 13, 15$ [$L = 8, 10, 12$], respectively.

to $\sum_{Z \ni i,j} \|\tilde{h}_Z\| \leq \tilde{\lambda}_0 \exp[-\frac{\tilde{\zeta}}{\tilde{\nu}} \text{dist}(i,j)^{\tilde{\kappa}}]$, Eq. (36) follows immediately.

DISCUSSION

Experimentally, both the realization of the quasiperiodic version of the programmable Rydberg chain [14] by additionally imposing, for instance, the site-resolved potential offset [21, 22] and the witness of OTOC and entanglement dynamics demand a high-fidelity local manipulation over the individual particles in analog quantum simulators by means of the techniques such as spin echoes, optical tweezers, Rydberg states, nuclear spins, trapped ions, and quantum gas microscopes [28–33]. Although tantalizingly challenging, direct detections of the characteristic double-logarithmic entanglement growth may still be attainable for cMBL using the developed protocols from Refs. [22, 34–36]. In parallel, it might be equally or

even more promising to probe the single-logarithmic build-up of the varied OTOCs as well as their power-law spatial decay to verify the cMBL phase and differentiate it from the dMBL and uMBL regimes.

To conclude, based on the experiment-inspired prototype minimal model, we computed the universal spacetime structures of OTOCs and LR bounds for the unconventional MBL states in constrained quantum spin systems. The OTOC inside the cMBL phase is characterized by a logarithmic temporal growth and a power-law spatial attenuation, whose light cone front is captured by a new LR bound which we derive. In comparison, the dMBL phase is featured by a power-law rise of OTOC, which decreases in space as per a stretched exponential function of separation. These findings, along with the established uMBL phase, potentially point towards an intrinsic organization of the fully MBL dynamical states of matter. Could it be that a parent theory would foster a comprehensive classification of the hierarchical variety of the unconventional MBL quantum dynamics and beyond? The unified description and continual elucidation of these challenges via exploiting the dynamics of quantum information may hold the prospect of enriching and advancing our current theoretical framework for localization.

METHODS

Out-of-time-order commutators

From the definition Eq. (1), it is easy to determine the following form of the out-of-time-order (OTO) commutator for the two Hermitian operators $A^\dagger(i, t) = A(i, t)$ and $B^\dagger(j, t) = B(j, t)$,

$$C_\beta^{AB}(i, j; t, t') = \langle [A(i, t), B(j, t')]^\dagger [A(i, t), B(j, t')] \rangle_\beta$$

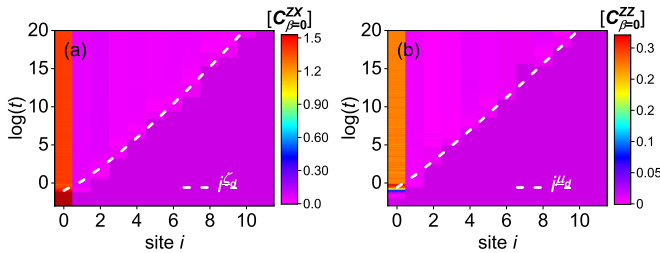


FIG. 5. The dMBL's light cones via $[C_{\beta=0}^{ZX}]$ and $[C_{\beta=0}^{ZZ}]$ using OBCs. The Hamiltonian parameters are the same as in Fig. 4. The two power-law fitting exponents are both greater than 1 with $\zeta_d \approx 1.228$ and $\mu_d \approx 1.107$.

$$\begin{aligned}
&= \langle B(j, t')A(i, t)A(i, t)B(j, t') \rangle_\beta \\
&+ \langle A(i, t)B(j, t')B(j, t')A(i, t) \rangle_\beta \\
&- 2\langle A(i, t)B(j, t')A(i, t)B(j, t') \rangle_\beta, \quad (37)
\end{aligned}$$

where $\langle \mathcal{O} \rangle_\beta = \text{Tr}[e^{-\beta H_{\text{ap}}} \mathcal{O}] / \text{Tr}[e^{-\beta H_{\text{ap}}}]$ and in the last line the cyclic property of the trace is used. If, in addition, the Hermitian operators are unitary as well, i.e., $A^2(i, t) = B^2(j, t) = \mathbb{1}$, then

$$C_\beta^{AB}(i, j; t, t') = 2 - 2F_\beta^{AB}(i, j; t, t') \quad (38)$$

with the OTO correlator defined by

$$F_\beta^{AB}(i, j; t, t') = \langle A(i, t)B(j, t')A(i, t)B(j, t') \rangle_\beta, \quad (39)$$

which is apparently real in this case.

However, owing to the fact that within the projected Hilbert space, \forall site i , $\tilde{X}_i^2 \neq \mathbb{1}$, the OTO commutators might not be exactly the same as the OTO correlators up to some constants. We are therefore chiefly relying on the general formula (37) throughout the numerical evaluation of the various OTO commutators for the constrained Rydberg array.

Exact diagonalization

The intertwined complications of the many-body nonequilibrium problem that stem from the superposed effects of constraint and randomness can be coped with by exact diagonalization method for small 1D finite systems. We resort to the standard full diagonalization algorithm to access the long-time behaviours of OTOCs, where the quadruple precision is implemented for achieving the time evolution up to $t \approx 10^{20}$. Within full diagonalization, the infinite-time limit can be resolved by invoking the diagonal approximation.

Furthermore, instead of iteratively removing the $\downarrow\downarrow$ -motifs from the unconstrained Hilbert space, we succeed in manufacturing the projected spin-1/2 basis in terms of a selected set of binary numbers via explicitly conforming to the constraint rule using straightforward combinatorial reasoning, which proves to be efficient for reaching larger system sizes.

For short to intermediate time scales, for instance, $t \sim 10^3 - 10^4$, one can optionally choose the Krylov-space iterative technique (viz., a variant of the familiar Lanczos method with the full reorthogonalization for prolonged time evolution) supplemented by the dynamical quantum typicality [37, 38] to quasixactly calculate $C_\beta^{AB}(i, j; t, t')$ according to the following approximation,

$$C_{\beta=0}^{AB}(i, j; t, t') \approx \langle \tilde{\psi} | [A(i, t), B(j, t')]^\dagger [A(i, t), B(j, t')] | \tilde{\psi} \rangle, \quad (40)$$

where the single pure state $|\tilde{\psi}\rangle$ is normalized and drawn randomly from the enormous unit hypersphere (of dimension

about twice larger than that of the Hilbert space) by a Haar measure, i.e., the uniform probability distribution over the surface of the hypersphere. Besides enabling the Krylov-type methods, one advantage of deploying Eq. (40) is that the standard deviation of the errors associated to the typicality approximation drops exponentially with the total Hilbert-space dimension. Without heavy parallel computation, we find that Eq. (40) can be readily implemented for the constrained model up to $L = 29$ under PBCs (the corresponding Hilbert-space size is 1149851) irrespective of whether the system is MBL, thermal, or critical (data will be shown elsewhere), thereby validating the applicability of this numerical means for OTOCs and other physical quantities of interest.

Hastings-Koma series

To derive the LR bound for the cMBL phase [Eq. (34)], we mainly borrow the general tactic of Hastings and Koma [24] to exploit the nontrivial consequences derived from the locality structure of the quantum many-body system when it is subject to the constraint as well as the irregularities. In particular, when deciphering the OTOC constructions, rather than working with the bare lattice Hamiltonian, we reformulate a modified Hastings-Koma series using the integral-of-motion representation, which makes it possible to upgrade the original scheme from the few-body interactions in an ergodic situation to the k -body interactions suitable for the context of cMBL. This technical improvement may find use during future applications.

DATA AVAILABILITY

The data set that supports the findings of the present study can be available from the corresponding authors via email upon reasonable request.

ACKNOWLEDGEMENTS

This work is supported by the National Key Research and Development Program of China (Grants Nos. 2017YFA0304204 and 2016YFA0300504), the National Natural Science Foundation of China Grant No. 11625416, and the Shanghai Municipal Government (Grants Nos. 19XD1400700 and 19JC1412702).

AUTHOR CONTRIBUTIONS

All authors contributed equally to this work.

COMPETING INTERESTS

The authors declare no competing financial or non-financial interests.

[1] P. W. Anderson, Absence of diffusion in certain random lattices, *Phys. Rev.* **109**, 1492 (1958).

[2] D. Basko, I. Aleiner, and B. Altshuler, Metal-insulator transition in a weakly interacting many-electron system with local-

- ized single-particle states, *Ann. Phys. (Amsterdam)* **321**, 1126 (2006).
- [3] I. V. Gornyi, A. D. Mirlin, and D. G. Polyakov, Interacting electrons in disordered wires: Anderson localization and low- T transport, *Phys. Rev. Lett.* **95**, 206603 (2005).
- [4] D. A. Abanin, E. Altman, I. Bloch, and M. Serbyn, Colloquium: Many-body localization, thermalization, and entanglement, *Rev. Mod. Phys.* **91**, 021001 (2019).
- [5] J. H. Bardarson, F. Pollmann, and J. E. Moore, Unbounded growth of entanglement in models of many-body localization, *Phys. Rev. Lett.* **109**, 017202 (2012).
- [6] R. Fan, P. Zhang, H. Shen, and H. Zhai, Out-of-time-order correlation for many-body localization, *Science Bulletin* **62**, 707 (2017).
- [7] Y. Huang, Y.-L. Zhang, and X. Chen, Out-of-time-ordered correlators in many-body localized systems, *Annalen der Physik* **529**, 1600318 (2016).
- [8] D. A. Huse, R. Nandkishore, and V. Oganesyan, Phenomenology of fully many-body-localized systems, *Phys. Rev. B* **90**, 174202 (2014).
- [9] M. Serbyn, Z. Papić, and D. A. Abanin, Local conservation laws and the structure of the many-body localized states, *Phys. Rev. Lett.* **111**, 127201 (2013).
- [10] M. van Horssen, E. Levi, and J. P. Garrahan, Dynamics of many-body localization in a translation-invariant quantum glass model, *Phys. Rev. B* **92**, 100305 (2015).
- [11] N. Pancotti, G. Giudice, J. I. Cirac, J. P. Garrahan, and M. C. Bañuls, Quantum east model: Localization, nonthermal eigenstates, and slow dynamics, *Phys. Rev. X* **10**, 021051 (2020).
- [12] A. Smith, J. Knolle, D. L. Kovrizhin, and R. Moessner, Disorder-free localization, *Phys. Rev. Lett.* **118**, 266601 (2017).
- [13] M. Brenes, M. Dalmonte, M. Heyl, and A. Scardicchio, Many-body localization dynamics from gauge invariance, *Phys. Rev. Lett.* **120**, 030601 (2018).
- [14] H. Bernien, S. Schwartz, A. Keesling, H. Levine, A. Omran, H. Pichler, S. Choi, A. S. Zibrov, M. Endres, M. Greiner, V. Vuletić, and M. D. Lukin, Probing many-body dynamics on a 51-atom quantum simulator, *Nature (London)* **551**, 579 (2017).
- [15] C. Chen, F. Burnell, and A. Chandran, How does a locally constrained quantum system localize?, *Phys. Rev. Lett.* **121**, 085701 (2018).
- [16] C. Chen, Y. Chen, and X. Wang, Many-body localization in the infinite-interaction limit and the discontinuous eigenstate phase transition, [arXiv:2011.09202](https://arxiv.org/abs/2011.09202) (2020).
- [17] E. H. Lieb and D. W. Robinson, The finite group velocity of quantum spin systems, *Commun. Math. Phys.* **28**, 251 (1972).
- [18] A. I. Larkin and Y. N. Ovchinnikov, Quasiclassical Method in the Theory of Superconductivity, *Sov. Phys. JETP* **28**, 120 (1969).
- [19] A. Kitaev, A simple model of quantum holography, [Talks presented at the Kavli Institute for Theoretical Physics, University of California, Santa Barbara \(7 April 2015 and 27 May 2015\)](https://www.kavli.ucsb.edu/sites/default/files/2015-04/1507.01450v2.pdf).
- [20] P. Hosur, X.-L. Qi, D. A. Roberts, and B. Yoshida, Chaos in quantum channels, *Journal of High Energy Phys.* **02**, 004 (2016).
- [21] M. Schreiber, S. S. Hodgman, P. Bordia, H. P. Lüschen, M. H. Fischer, R. Vosk, E. Altman, U. Schneider, and I. Bloch, Observation of many-body localization of interacting fermions in a quasirandom optical lattice, *Science* **349**, 842 (2015).
- [22] A. Lukin, M. Rispoli, R. Schittko, M. E. Tai, A. M. Kaufman, S. Choi, V. Khemani, J. Léonard, and M. Greiner, Probing entanglement in a many-body-localized system, *Science* **364**, 256 (2019).
- [23] I. H. Kim, A. Chandran, and D. A. Abanin, Local integrals of motion and the logarithmic lightcone in many-body localized systems, [arXiv:1412.3073](https://arxiv.org/abs/1412.3073) (2014).
- [24] M. B. Hastings and T. Koma, Spectral Gap and Exponential Decay of Correlations, *Commun. Math. Phys.* **265**, 781 (2006).
- [25] M. Foss-Feig, Z.-X. Gong, C. W. Clark, and A. V. Gorshkov, Nearly Linear Light Cones in Long-Range Interacting Quantum Systems, *Phys. Rev. Lett.* **114**, 157201 (2015).
- [26] See Supplementary Information for the analytical derivation and the additional numerical materials.
- [27] S. Bravyi, M. B. Hastings, and F. Verstraete, Lieb-Robinson Bounds and the Generation of Correlations and Topological Quantum Order, *Phys. Rev. Lett.* **97**, 050401 (2006).
- [28] J. Li, R. Fan, H. Wang, B. Ye, B. Zeng, H. Zhai, X. Peng, and J. Du, Measuring out-of-time-order correlators on a nuclear magnetic resonance quantum simulator, *Phys. Rev. X* **7**, 031011 (2017).
- [29] M. Garttner, J. G. Bohnet, A. Safavi-Naini, M. L. Wall, J. J. Bollinger, and A. M. Rey, Measuring out-of-time-order correlations and multiple quantum spectra in a trapped-ion quantum magnet, *Nat. Phys.* **13**, 781 (2017).
- [30] E. J. Meier, J. Ang'ong'a, F. A. An, and B. Gadway, Exploring quantum signatures of chaos on a floquet synthetic lattice, *Phys. Rev. A* **100**, 013623 (2019).
- [31] K. A. Landsman, C. Figgatt, T. Schuster, N. M. Linke, B. Yoshida, N. Y. Yao, and C. Monroe, Verified quantum information scrambling, *Nature (London)* **567**, 61 (2019).
- [32] B. Swingle, G. Bentsen, M. Schleier-Smith, and P. Hayden, Measuring the scrambling of quantum information, *Phys. Rev. A* **94**, 040302 (2016).
- [33] K. X. Wei, C. Ramanathan, and P. Cappellaro, Exploring localization in nuclear spin chains, *Phys. Rev. Lett.* **120**, 070501 (2018).
- [34] A. M. Kaufman, M. E. Tai, A. Lukin, M. Rispoli, R. Schittko, P. M. Preiss, and M. Greiner, Quantum thermalization through entanglement in an isolated many-body system, *Science* **353**, 794 (2016).
- [35] T. Brydges, A. Elben, P. Jurcevic, B. Vermersch, C. Maier, B. P. Lanyon, P. Zoller, R. Blatt, and C. F. Roos, Probing Rényi entanglement entropy via randomized measurements, *Science* **364**, 260 (2019).
- [36] J. Smith, A. Lee, P. Richerme, B. Neyenhuis, P. W. Hess, P. Hauke, M. Heyl, D. A. Huse, and C. Monroe, Many-body localization in a quantum simulator with programmable random disorder, *Nat. Phys.* **12**, 907 (2016).
- [37] S. Goldstein, J. L. Lebowitz, R. Tumulka, and N. Zanghì, Canonical typicality, *Phys. Rev. Lett.* **96**, 050403 (2006).
- [38] S. Popescu, A. J. Short, and A. Winter, Entanglement and the foundations of statistical mechanics, *Nat. Phys.* **2**, 754 (2006).

Supplementary Information for “Lieb-Robinson bound for constrained many-body localization”

Chun Chen,^{1,*} Xiaoqun Wang,^{2,3,4,†} and Yan Chen^{5,6,‡}

¹Max-Planck-Institut für Physik komplexer Systeme, Nöthnitzer Straße 38, 01187 Dresden, Germany

²Key Laboratory of Artificial Structures and Quantum Control of MOE,
Shenyang National Laboratory for Materials Science, Shenyang 110016, China

³School of Physics and Astronomy, Tsung-Dao Lee Institute,
Shanghai Jiao Tong University, Shanghai 200240, China

⁴Beijing Computational Science Research Center, Beijing 100084, China

⁵Department of Physics and State Key Laboratory of Surface Physics, Fudan University, Shanghai 200433, China

⁶Collaborative Innovation Center of Advanced Microstructures, Nanjing University, Nanjing 210093, China

(Dated: May 3, 2022)

S1. THE HAMILTONIAN IN THE INTEGRALS-OF-MOTION REPRESENTATION

It is an obvious fact that a simple, local, short-range, few-body Hamiltonian will typically acquire a very complicated, non-local, long-range, k -body form when rewritten in the representation of the integrals of motion. For example, assume the lattice system is described by the following Hamiltonian,

$$H = \sum_{\{j,N\}} h_{\{j,N\}}, \quad (\text{S1})$$

where $h_{\{j,N\}}$ is a locally interacting term centred on site j and contains operators up to the N th nearest neighbours of j . Now introducing the unitary matrix U that diagonalizes the matrix of the operator H in a chosen basis, i.e.,

$$[UHU^\dagger]_{n',n} = \langle n'|H|n\rangle = E_n \langle n'|n\rangle = E_n \delta_{n',n}. \quad (\text{S2})$$

Then, in terms of the eigenenergies and the eigenstates, this relation simply means that

$$H = \sum_{\{j,N\}} \sum_n \langle n|h_{\{j,N\}}|n\rangle |n\rangle \langle n| = \sum_n E_n |n\rangle \langle n|, \quad (\text{S3})$$

where $\{\sum_n \langle n|h_{\{j,N\}}|n\rangle |n\rangle \langle n|\}$ comprises the set of integrals of motion of the system, as they are not only mutually commuting but also commute with H . Normally, $\sum_n \langle n|h_{\{j,N\}}|n\rangle |n\rangle \langle n|$ is a highly nonlocal and k -body interacting term in the typical circumstances.

Specialize to the case of the unconstrained many-body-localized (uMBL) models, a widely-adopted theoretical framework to explain the breakdown of ergodicity there is based on the notion of the so-called (quasi)local integrals of motion. Take, for instance, a general locally interacting spin-1/2 chain with randomness along z -direction, then according to this formalism, it is phenomenologically deduced that when the system is deeply inside the fully uMBL phase, the effective Hamiltonian matrix assumes

$$H_{\text{uMBL}} = \sum_i \tilde{h}_i \tau_i^z + \sum_{i>j} J_{ij} \tau_i^z \tau_j^z + \sum_{i>j>k} J_{ijk} \tau_i^z \tau_j^z \tau_k^z + \dots, \quad (\text{S4})$$

where $\{\tau_i^z\}_{n',n} := [U\sigma_i^z U^\dagger]_{n',n}$ comprises another set of quasilocal integrals of motion built from the physical spins $\{\sigma_i^z\}$ by the quasilocal unitary matrix U , which further implies that the various k -body interaction strengths $\{\tilde{h}_i, J_{ij}, J_{ijk}, \dots\}$ should decay rapidly in space.

* Corresponding author: chun6@pks.mpg.de

† Corresponding author.
xiaoqunwang@sjtu.edu.cn

‡ Corresponding author: yanchen99@fudan.edu.cn

S2. DIVIDING THE HAMILTONIAN INTO SHORT-RANGE AND LONG-RANGE PARTS

After writing the local and finite-range Hamiltonian into a nonlocal and infinite-range form,

$$H = \sum_{\{j,N\}} h_{\{j,N\}} = \sum_{\{j,N\}} \tilde{h}_{\{j,N\}}, \quad (\text{S5})$$

where the integrals of motion are defined by

$$\tilde{h}_{\{j,N\}} := \sum_n \langle n | h_{\{j,N\}} | n \rangle | n \rangle \langle n |, \quad (\text{S6})$$

one can proceed to separate H into the short-range and the long-range pieces via imposing a dynamical length scale χ . Namely,

$$H = \sum_Z \tilde{h}_Z = \sum_{Z^{sr}} \tilde{h}_{Z^{sr}} + \sum_{Z^{lr}} \tilde{h}_{Z^{lr}}. \quad (\text{S7})$$

Here, any individual terms of $\{\tilde{h}_Z\}$ that are supported exclusively on a lattice subset fulfilling $\text{diam}(Z^{sr}) \leq \chi$ are grouped into the short-range part $\sum_{Z^{sr}} \tilde{h}_{Z^{sr}}$. All the remaining terms are then classified as the long-range part $\sum_{Z^{lr}} \tilde{h}_{Z^{lr}}$. Note that each \tilde{h}_Z might resemble H in expression but they cannot be reduced to h_Z because besides commuting with H , $\{\tilde{h}_Z\}$ themselves also mutually commute.

S3. THE INTERACTION PICTURE

The main purpose of invoking Eq. (S7) is to transform the formulation of the Lieb-Robinson (LR) bound from the original Heisenberg picture to the interaction picture such that one is not only endowed with a variable length scale χ to tune but is also able to derive its meaningful form through the manipulation of the standard Hastings-Koma (HK) series. So, let's first introduce the apparatus of the interaction picture.

In order to be compatible with the OTOC results, we assume that the k -body Hamiltonian for the constrained MBL (cMBL) phase,

$$H_\Lambda = \sum_{Z \subset \Lambda_s} \tilde{h}_Z, \quad (\text{S8})$$

satisfies three conditions.

(i) The power-law decaying interactions, i.e.,

$$\sum_{Z \ni x,y} \|\tilde{h}_Z\| \leq \frac{\lambda_0}{[1 + \text{dist}(x,y)]^\eta}, \quad (\text{S9})$$

for any fixed site indices x and y .

(ii) The reproducing condition,

$$\sum_{z \in \Lambda_s} \frac{1}{[1 + \text{dist}(x,z)]^\eta} \frac{1}{[1 + \text{dist}(z,y)]^\eta} \leq \frac{p_0}{[1 + \text{dist}(x,y)]^\eta}. \quad (\text{S10})$$

(iii) Related to the reproducing condition, it is assumed that

$$\sup_{\Lambda_s} \sup_x \sum_{y \in \Lambda_s} \frac{1}{[1 + \text{dist}(x,y)]^\eta} = s' < \infty. \quad (\text{S11})$$

Here, positive constants λ_0, η, p_0, s' are independent of the volume of Λ_s , the underlying lattice system of sites and bonds.

In accord with Eq. (S7), the k -body interacting Hamiltonian (S8) is rewritten as follows,

$$H_\Lambda = H_\Lambda^{sr} + H_\Lambda^{lr}, \quad (\text{S12})$$

where

$$H_{\Lambda}^{sr} = \sum_{\substack{Z^{sr}: Z^{sr} \subset \Lambda_s \\ \text{diam}(Z^{sr}) \leq \chi}} \tilde{h}_{Z^{sr}} \quad \text{and} \quad H_{\Lambda}^{lr} = \sum_{\substack{Z^{lr}: Z^{lr} \subset \Lambda_s \\ \text{diam}(Z^{lr}) > \chi}} \tilde{h}_{Z^{lr}}. \quad (\text{S13})$$

Next, we recap the major formulas in different pictures. Throughout the derivation we always set $\hbar = 1$. First, take A as a generic time-independent Schrödinger operator, then in the Heisenberg representation governed by H_{Λ} , it becomes

$$A_H(t) = e^{iH_{\Lambda}t} A e^{-iH_{\Lambda}t}. \quad (\text{S14})$$

Instead, if choosing to evolve with just H_{Λ}^{sr} , one leads to the interaction-picture operator,

$$A_I(t) = e^{iH_{\Lambda}^{sr}t} A e^{-iH_{\Lambda}^{sr}t}. \quad (\text{S15})$$

It is easy to recognize the unitary scattering-matrix operator that connects the interaction picture to the Heisenberg picture,

$$A_H(t) = \mathcal{S}^{\dagger}(t) A_I(t) \mathcal{S}(t), \quad \mathcal{S}(t) = e^{iH_{\Lambda}^{sr}t} e^{-iH_{\Lambda}t}, \quad (\text{S16})$$

whose form can be derived from its equation of motion,

$$\frac{d\mathcal{S}(t)}{dt} = H_{\Lambda, I}^{lr}(t) \mathcal{S}(t), \quad H_{\Lambda, I}^{lr}(t) = e^{iH_{\Lambda}^{sr}t} H_{\Lambda}^{lr} e^{-iH_{\Lambda}^{sr}t}, \quad (\text{S17})$$

as the following,

$$\mathcal{S}(t) = \sum_{n=0}^{\infty} \left(-\frac{i}{\hbar}\right)^n \frac{1}{n!} \int_0^t dt_1 \cdots \int_0^{t_1} dt_n T[H_{\Lambda, I}^{lr}(t_1) H_{\Lambda, I}^{lr}(t_2) \cdots H_{\Lambda, I}^{lr}(t_n)]. \quad (\text{S18})$$

We start to analyze the short-range contribution to the LR bound from H_{Λ}^{sr} . Let A, B be two observables supported on the compact sets, $X, Y \subset \Lambda_s$. The standard HK series gives

$$\begin{aligned} \frac{\|[A_I(t), B]\|}{\|A\|} &\leq 2\|B\|(2|t|) \sum_{\substack{Z_1^{sr}: Z_1^{sr} \cap X \neq \emptyset \\ Z_1^{sr} \cap Y \neq \emptyset}} \|\tilde{h}_{Z_1^{sr}}\| + 2\|B\| \frac{(2|t|)^2}{2!} \sum_{Z_1^{sr}: Z_1^{sr} \cap X \neq \emptyset} \|\tilde{h}_{Z_1^{sr}}\| \sum_{\substack{Z_2^{sr}: Z_2^{sr} \cap Z_1^{sr} \neq \emptyset \\ Z_2^{sr} \cap Y \neq \emptyset}} \|\tilde{h}_{Z_2^{sr}}\| \\ &+ 2\|B\| \frac{(2|t|)^3}{3!} \sum_{Z_1^{sr}: Z_1^{sr} \cap X \neq \emptyset} \|\tilde{h}_{Z_1^{sr}}\| \sum_{Z_2^{sr}: Z_2^{sr} \cap Z_1^{sr} \neq \emptyset} \|\tilde{h}_{Z_2^{sr}}\| \sum_{\substack{Z_3^{sr}: Z_3^{sr} \cap Z_2^{sr} \neq \emptyset \\ Z_3^{sr} \cap Y \neq \emptyset}} \|\tilde{h}_{Z_3^{sr}}\| + \cdots \end{aligned} \quad (\text{S19})$$

By exploiting Eqs. (S9), (S10), and (S11), one can simplify the terms of (S19) as follows,

$$\sum_{\substack{Z_1^{sr}: Z_1^{sr} \cap X \neq \emptyset \\ Z_1^{sr} \cap Y \neq \emptyset}} \|\tilde{h}_{Z_1^{sr}}\| \leq \sum_{x \in X} \sum_{y \in Y} \sum_{Z_1^{sr} \ni x, y} \|\tilde{h}_{Z_1^{sr}}\| \leq \sum_{x \in X} \sum_{y \in Y} \frac{\lambda_0}{[1 + \text{dist}(x, y)]^{\eta}} \leq \sum_{x \in X} \lambda_0 s' = |X| \lambda_0 s'. \quad (\text{S20})$$

For the second term,

$$\begin{aligned} \sum_{Z_1^{sr}: Z_1^{sr} \cap X \neq \emptyset} \|\tilde{h}_{Z_1^{sr}}\| \sum_{\substack{Z_2^{sr}: Z_2^{sr} \cap Z_1^{sr} \neq \emptyset \\ Z_2^{sr} \cap Y \neq \emptyset}} \|\tilde{h}_{Z_2^{sr}}\| &\leq \sum_{x \in X} \sum_{y \in Y} \sum_{z_{12} \in \Lambda_s} \sum_{Z_1^{sr} \ni x, z_{12}} \|\tilde{h}_{Z_1^{sr}}\| \sum_{Z_2^{sr} \ni z_{12}, y} \|\tilde{h}_{Z_2^{sr}}\| \\ &\leq \sum_{x \in X} \sum_{y \in Y} \sum_{z_{12} \in \Lambda_s} \frac{\lambda_0}{[1 + \text{dist}(x, z_{12})]^{\eta}} \frac{\lambda_0}{[1 + \text{dist}(z_{12}, y)]^{\eta}} \\ &\leq \sum_{x \in X} \sum_{y \in Y} \frac{\lambda_0^2 p_0}{[1 + \text{dist}(x, y)]^{\eta}} = |X| \lambda_0^2 p_0 s'. \end{aligned} \quad (\text{S21})$$

Proceed analogously for the higher-order terms, one arrives at

$$\frac{\|[A_I(t), B]\|}{\|A\|} \leq 2\|B\| |X| p_0^{-1} s' \left(2|t| \lambda_0 p_0 + \frac{(2|t| \lambda_0 p_0)^2}{2!} + \frac{(2|t| \lambda_0 p_0)^3}{3!} + \cdots \right)$$

$$\begin{aligned}
&\leq 2\|B\|\|X\|p_0^{-1}s' \sum_{a=\lceil r/\chi \rceil}^{\infty} \frac{(2|t|\lambda_0 p_0)^a}{a!}; \quad r = \text{dist}(X, Y) \\
&\leq 2\|B\|\|X\|p_0^{-1}s' \sum_{a=\lceil r/\chi \rceil}^{\infty} \frac{(2|t|\lambda_0 p_0)^a}{a!} e^{a-\lceil r/\chi \rceil} \leq 2\|B\|\|X\|p_0^{-1}s' \sum_{a=0}^{\infty} \frac{(2|t|e\lambda_0 p_0)^a}{a!} e^{-\lceil r/\chi \rceil} \\
&\leq 2\|B\|\|X\|p_0^{-1}s' \exp(2|t|e\lambda_0 p_0 - r/\chi), \tag{S22}
\end{aligned}$$

where in the second line, we use the observation that the range of H_Λ^{sr} is within χ so that the HK sequence in Eq. (S19) needs at least $\lceil r/\chi \rceil$ iterations to bridge regions X and Y , but in the final steps of (S22) we still add back these contributions to get a closed expression.

Define the LR velocity for the short-range interactions,

$$v = 2e\lambda_0 p_0, \tag{S23}$$

Eq. (S22) is repeated by

$$\frac{\|[A_I(t), B]\|}{\|A\|} \leq 2\|B\|\|X\|p_0^{-1}s' \exp(v|t| - r/\chi), \tag{S24}$$

where picking up a threshold ε_0 gives rise to the definition of the radius $R(t)$ of the short-range linear lightcone,

$$r = \chi v|t| - \chi \varepsilon_0 \implies R(t) = \chi v|t|. \tag{S25}$$

A common practice of using the result (S24) is to approximate the long-range operator $A_I(t)$ by a sequence of intermediate operators whose supports, although expanding, are strictly finite-ranged. Following Refs. [1, 2], $\mathbb{B}[X, R_\ell(t)]$ denotes a ball of radius $R_\ell(t) = R(t) + \ell\chi$, $\ell = 0, 1, 2, \dots$, centred on set X ,

$$\mathbb{B}[X, R_\ell(t)] := \{i \in \Lambda_s | \text{dist}(i, X) \leq R_\ell(t)\}. \tag{S26}$$

By an integration over the unitary group equipped with the Haar measure, the content of $A_I(t)$ confined within $\mathbb{B}[X, R_\ell(t)]$ can be formally isolated,

$$A_I(\ell, t) := e^{iH_\Lambda^{sr}t} \left\{ \int_{\overline{\mathbb{B}[X, R_\ell(0)]}} d\mu(U) U A U^\dagger \right\} e^{-iH_\Lambda^{sr}t}, \tag{S27}$$

where $\overline{\mathbb{B}[X, R_\ell(t)]}$ is the complement of $\mathbb{B}[X, R_\ell(t)]$ with respect to Λ_s , i.e., operator $A_I(\ell, t)$ has no support outside the ball $\mathbb{B}[X, R(t) + \ell\chi(0)]$.

The usefulness of $\{A_I(\ell, t)\}$ resides in their resemblance to $A_I(t)$ in the sense that

$$\begin{aligned}
\|A_I(\ell, t) - A_I(t)\| &= \left\| e^{iH_\Lambda^{sr}t} \left\{ \int_{\overline{\mathbb{B}[X, R_\ell(0)]}} d\mu(U) [U A U^\dagger - A U U^\dagger] \right\} e^{-iH_\Lambda^{sr}t} \right\| \\
&\leq \int_{\overline{\mathbb{B}[X, R_\ell(0)]}} d\mu(U) \|[U A - A U] U^\dagger\| = \int_{\overline{\mathbb{B}[X, R_\ell(0)]}} d\mu(U) \|[A, U]\| \\
&\leq 2\|A\|\|U\|\|X\|p_0^{-1}s' \exp[-R_\ell(0)/\chi(0)] = 2\|A\|\|X\|p_0^{-1}s' \exp(-\ell), \tag{S28}
\end{aligned}$$

where inequality (S24) has been inserted and $\chi(0)$ should be understood as $\chi(t \rightarrow 0^+)$. Due to the exponential reduction of the deviation as a function of ℓ , when $\ell \rightarrow \infty$, $A_I(\infty, t)$ approaches $A_I(t)$ to a good approximation. Define next

$$A_I^0(t) = A_I(0, t), \quad A_I^{\ell>0}(t) = A_I(\ell, t) - A_I(\ell - 1, t), \tag{S29}$$

then clearly

$$A_I(t) = A_I(0, t) + \sum_{\ell=1}^{\infty} [A_I(\ell, t) - A_I(\ell - 1, t)] = \sum_{\ell=0}^{\infty} A_I^\ell(t). \tag{S30}$$

Accordingly, relation (S28) implies that for $\ell > 0$,

$$\begin{aligned} \|A_I^\ell(t)\| &= \|A_I(\ell, t) - A_I(t) - [A_I(\ell - 1, t) - A_I(t)]\| \\ &\leq \|A_I(\ell, t) - A_I(t)\| + \|A_I(\ell - 1, t) - A_I(t)\| \leq 2\|A\| |X| p_0^{-1} s' (1 + e) \exp(-\ell). \end{aligned} \quad (\text{S31})$$

Instead, for $\ell = 0$,

$$\|A_I^0(t)\| \leq \|A_I(0, t) - A_I(t)\| + \|A_I(t)\| \leq 2\|A\| |X| p_0^{-1} s' + \|A\|. \quad (\text{S32})$$

Note that if $2|X|p_0^{-1}s'e \geq 1$, then $\|A_I^0(t)\| \leq 2\|A\||X|p_0^{-1}s'(1+e)$. In comparison, if $\|A\| \geq 2|X|p_0^{-1}s'e\|A\|$, then the decay of the norm is even faster than the exponential for the first term.

Thus, as emphasized in Ref. [2], one shall in principle find a way to write $A_I(t)$ as a sum of a sequence of operator $A_I^\ell(t)$ with increasing (and finite) support but exponentially decreasing bounds of the norm. This examination of the short-range interactions exemplifies the core content and the meaning of the employment of the interaction-picture formulation for deriving the LR bound.

S4. INCORPORATE LONG-RANGE INTERACTIONS IN THE INTERACTION PICTURE

Our main target is the LR bound for the Heisenberg operators, therefore in terms of the scattering-matrix operator, it is easy to see that

$$\|[A_H(t), B]\| = \|[A_I(t), \mathcal{S}(t)B\mathcal{S}^\dagger(t)]\| \leq \sum_{\ell=0}^{\infty} \|[A_I^\ell(t), \mathcal{S}(t)B\mathcal{S}^\dagger(t)]\|. \quad (\text{S33})$$

Following [2], the overall strategy of tackling (S33) is to employ the interaction-picture equation of motion for $\mathcal{S}(t)$ to write a first-order differential equation for the relevant commutator defined below, and then the obtained result is converted into a HK-like integral equation that can be iterated to include the contributions from the long-range interactions in a progressive manner and thus produce the desired sequence of the full LR bound. Recall that H_Λ^{lr} has been exclusively encapsulated in $\mathcal{S}(t)$.

Now, let's introduce the generalized two-time commutator,

$$G_r^\ell(t, \tau) := [A_I^\ell(t), \mathcal{S}(\tau)B\mathcal{S}^\dagger(\tau)], \quad r := \text{dist}(X, Y). \quad (\text{S34})$$

Then, applying Eq. (S17) yields,

$$\frac{dG_r^\ell(t, \tau)}{d\tau} = -i [A_I^\ell(t), [H_{\Lambda, I}^{lr}(\tau), \mathcal{S}(\tau)B\mathcal{S}^\dagger(\tau)]]. \quad (\text{S35})$$

Implementing the same decomposition like that of Eq. (S30) for the long-range Hamiltonian,

$$H_{\Lambda, I}^{lr}(\tau) = \sum_{Z^{lr}} \sum_{m=0}^{\infty} \tilde{h}_{Z^{lr}, I}^m(\tau), \quad (\text{S36})$$

where for each Z^{lr} , there arises a corresponding summation index $m_{Z^{lr}}$ whose subscript has been omitted in (S36) for brevity. Then, it is easy to notice that the nested commutator is nonzero only if there exist some m 's such that

$$\mathbb{B}[A_I^\ell(t)] \cap \mathbb{B}[\tilde{h}_{Z^{lr}, I}^m(\tau)] \neq \emptyset. \quad (\text{S37})$$

Nonetheless, the mismatch between the arguments t and τ renders the execution of this crucial condition very complicated in the ensuing HK iterations. More importantly, Eq. (S37) is the key resource where the explicit t -dependence can be extracted for modifying the LR bound. To this end, one would like to inquire whether there exists the kind of relations like the following,

$$\mathbb{B}[A_I^\ell(t)] \cap \mathbb{B}[\tilde{h}_{Z^{lr}, I}^m(\tau)] \neq \emptyset \implies \mathbb{B}[A_I^\ell(t)] \cap \mathbb{B}[\tilde{h}_{Z^{lr}, I}^m(t)] \neq \emptyset? \quad (\text{S38})$$

As we now show, the answer is affirmative for the primary cases that interest us. The trick here is to utilize the familiar identity that for arbitrary operator A and any unitary operator U ,

$$\|A\| = \|UAU^\dagger\|, \quad (\text{S39})$$

to shift the t -argument in the definition (S15) of the interaction-picture operators. Concretely, for two arbitrary interaction-picture operators, one can prove that

$$\|[A_I(t), B_I(\tau)]\| = \|[A_I(t + \Delta t), B_I(\tau + \Delta t)]\|, \quad (\text{S40})$$

where the essential requirements are (1) $A_I(t)$ and $B_I(\tau)$ have to be defined by the same short-range Hamiltonian H_Λ^{sr} and (2) Schrödinger operators A, B themselves are independent of time. Apparently, truncated operators generated by (S27) fulfill these two conditions.

The proof is divided into two parts: (I) the growing balls and (II) the shrinking balls.

I. In the case of expanding balls, it is relatively easy to appreciate that based on

$$\mathbb{B}[A_I(\tau)] \cap \mathbb{B}[B_I(\tau')] \neq \emptyset, \quad (\text{S41})$$

where $0 \leq \tau', \tau \leq t$, one can safely pretend that this condition implies

$$\mathbb{B}[A_I(t)] \cap \mathbb{B}[B_I(t)] \neq \emptyset, \quad (\text{S42})$$

because the added contributions from extending the time domains are precisely compensated by the associated commutators (see below) which vanish identically in these enlarged regions of the balls. In other words, nothing extra has been included in essence. It is worth mentioning that this seemingly elementary extension from τ, τ' to t actually underpins the whole constructions of Ref. [2].

II. Because we concern the unconventional MBL, it is natural to anticipate that the balls or more precisely the dynamical length scale χ might be shrinking. For this circumstance, we proceed as follows: First,

$$[A_I(\tau), B_I(\tau')] \neq \emptyset \implies \|[A_I(\tau), B_I(\tau')]\| \neq 0. \quad (\text{S43})$$

Then, shifting the arguments τ, τ' by $t - \tau'$ as per (S40),

$$\|[A_I(\tau), B_I(\tau')]\| = \|[A_I(\tau + t - \tau'), B_I(t)]\| \neq 0, \quad (\text{S44})$$

yields

$$\mathbb{B}[A_I(\tau)] \cap \mathbb{B}[B_I(\tau')] \neq \emptyset \implies \mathbb{B}[A_I(\tau + t - \tau')] \cap \mathbb{B}[B_I(t)] \neq \emptyset. \quad (\text{S45})$$

In the HK series (see below), typically

$$0 \leq \tau' \leq \tau \leq t \implies t \leq \tau + t - \tau' \leq \tau + t, \quad (\text{S46})$$

therefore, for the case of shrinking balls,

$$\mathbb{B}[A_I(\tau)] \cap \mathbb{B}[B_I(\tau')] \neq \emptyset \implies \mathbb{B}[A_I(t)] \cap \mathbb{B}[B_I(t)] \neq \emptyset \quad (\text{S47})$$

as desired. Apparently, Eq. (S47) cannot be true for arbitrary τ and τ' with respect to t .

Now let's turn to Eq. (S35), whose expression can be transformed by the Jacobi identity, $[A, [B, C]] + [B, [C, A]] + [C, [A, B]] = 0$, as

$$\begin{aligned} \frac{dG_r^\ell(t, \tau)}{d\tau} &= -i \sum_{Z^{lr}} \sum_{m=0}^{\infty} [\tilde{h}_{Z^{lr}, I}^m(\tau), [A_I^\ell(t), \mathcal{S}(\tau) B \mathcal{S}^\dagger(\tau)]] + i \sum_{Z^{lr}} \sum_{m=0}^{\infty} [\mathcal{S}(\tau) B \mathcal{S}^\dagger(\tau), [A_I^\ell(t), \tilde{h}_{Z^{lr}, I}^m(\tau)]] \\ &= -i \sum_{Z^{lr}} \sum_{m=0}^{\infty} [\tilde{h}_{Z^{lr}, I}^m(\tau), [A_I^\ell(t), \mathcal{S}(\tau) B \mathcal{S}^\dagger(\tau)]] + i \sum_{Z^{lr}} \sum_{m=0}^{\infty} \mathcal{D}_i(t; Z^{lr}, m) [\mathcal{S}(\tau) B \mathcal{S}^\dagger(\tau), [A_I^\ell(t), \tilde{h}_{Z^{lr}, I}^m(\tau)]], \end{aligned} \quad (\text{S48})$$

where we introduce a step-like function [2] as the knob to access the condition (S37),

$$\mathcal{D}_i(t; Z^{lr}, m) = \begin{cases} 1 & \text{if } \mathbb{B}[A_I^\ell(t)] \cap \mathbb{B}[\tilde{h}_{Z^{lr}, I}^m(t)] \neq \emptyset, \\ 0 & \text{otherwise.} \end{cases} \quad (\text{S49})$$

Implement again the Jacobi identity for the last term in Eq. (S48) gives

$$\frac{dG_r^\ell(t, \tau)}{d\tau} = -i [H_{\Lambda, I}^{lr}(\tau) - \tilde{H}_{\Lambda, I}^{lr}(t, \tau), G_r^{lr}(t, \tau)] - i [A_I^{lr}(t), [\tilde{H}_{\Lambda, I}^{lr}(t, \tau), \mathcal{S}(\tau) B \mathcal{S}^\dagger(\tau)]], \quad (\text{S50})$$

where we define

$$\tilde{H}_{\Lambda,I}^{lr}(t, \tau) := \sum_{Z^{lr}} \sum_{m=0}^{\infty} \mathcal{D}_i(t; Z^{lr}, m) \tilde{h}_{Z^{lr},I}^m(\tau). \quad (\text{S51})$$

Then, a standard inequality in the theory of first-order differential equation [3] applies to Eq. (S50) and leads to the HK series in the interaction picture for iteration,

$$\begin{aligned} \|[A_I^\ell(t), \mathcal{S}(t)BS^\dagger(t)]\| &\leq \|[A_I^\ell(t), B]\| + \int_0^t d\tau \|[A_I^\ell(t), [\tilde{H}_{\Lambda,I}^{lr}(t, \tau), \mathcal{S}(\tau)BS^\dagger(\tau)]]\| \\ &\leq \|[A_I^\ell(t), B]\| + \sum_{Z^{lr}, m} \mathcal{D}_i(t; Z^{lr}, m) \int_0^t d\tau \|[A_I^\ell(t), [\tilde{h}_{Z^{lr},I}^m(\tau), \mathcal{S}(\tau)BS^\dagger(\tau)]]\| \\ &\leq \|[A_I^\ell(t), B]\| + 2\|A_I^\ell(t)\| \sum_{Z^{lr}, m} \mathcal{D}_i(t; Z^{lr}, m) \int_0^t d\tau \|[\tilde{h}_{Z^{lr},I}^m(\tau), \mathcal{S}(\tau)BS^\dagger(\tau)]\|, \end{aligned} \quad (\text{S52})$$

where Eq. (S34) has been recalled and $\sum_{Z^{lr}, m}(\dots)$ stands for $\sum_{Z^{lr}} \sum_{m=0}^{\infty}(\dots)$. Next, after recognizing the resemblance between $\|[\tilde{h}_{Z^{lr},I}^m(\tau), \mathcal{S}(\tau)BS^\dagger(\tau)]\|$ and $\|[A_I^\ell(t), \mathcal{S}(t)BS^\dagger(t)]\|$, one might tend to start the iteration. A direct injection of the result (S52) leads to

$$\begin{aligned} \|[\tilde{h}_{Z^{lr},I}^m(\tau), \mathcal{S}(\tau)BS^\dagger(\tau)]\| &\leq \|[\tilde{h}_{Z^{lr},I}^m(\tau), B]\| \\ &\quad + 2\|\tilde{h}_{Z^{lr},I}^m(\tau)\| \sum_{Z_1^{lr}, m_1} \mathcal{D}(\tau; Z^{lr}, m; Z_1^{lr}, m_1) \int_0^\tau d\tau_1 \|[\tilde{h}_{Z_1^{lr},I}^{m_1}(\tau_1), \mathcal{S}(\tau_1)BS^\dagger(\tau_1)]\|, \end{aligned} \quad (\text{S53})$$

where the τ -dependence of $\mathcal{D}(\tau; Z^{lr}, m; Z_1^{lr}, m_1)$ is inconvenient and insufficient for simplifying the expression of the iteration as more and more different τ_i -dependence will be engendered. However, by going through the same derivations above, it is not hard to realize that $\mathcal{D}(\tau; Z^{lr}, m; Z_1^{lr}, m_1)$ can be simply replaced by $\mathcal{D}(t; Z^{lr}, m; Z_1^{lr}, m_1)$ in (S53).

For instance, within $0 \leq \tau' \leq \tau \leq t$, define

$$\tilde{G}_{\tilde{r}}^m(\tau, \tau') := [\tilde{h}_{Z^{lr},I}^m(\tau), \mathcal{S}(\tau')BS^\dagger(\tau')], \quad \tilde{r} := \text{dist}(Z^{lr}, Y). \quad (\text{S54})$$

Parallel calculation using Eqs. (S42) and (S47) yields

$$[\tilde{h}_{Z^{lr},I}^m(\tau), H_{\Lambda,I}^{lr}(\tau')] = \sum_{Z_1^{lr}, m_1} \mathcal{D}(t; Z^{lr}, m; Z_1^{lr}, m_1) [\tilde{h}_{Z^{lr},I}^m(\tau), \tilde{h}_{Z_1^{lr},I}^{m_1}(\tau')], \quad (\text{S55})$$

where a general step function is given by

$$\mathcal{D}(t; Z^{lr}, m; Z_1^{lr}, m_1) = \begin{cases} 1 & \text{if } \mathbb{B}[\tilde{h}_{Z^{lr},I}^m(t)] \cap \mathbb{B}[\tilde{h}_{Z_1^{lr},I}^{m_1}(t)] \neq \emptyset, \\ 0 & \text{otherwise.} \end{cases} \quad (\text{S56})$$

The resulting first-order differential equation of motion of \tilde{G} is thus

$$\begin{aligned} \frac{d\tilde{G}_{\tilde{r}}^m(\tau, \tau')}{d\tau'} &= -i[H_{\Lambda,I}^{lr}(\tau') - \tilde{H}_{\Lambda,I}^{Z^{lr},m}(t, \tau'), \tilde{G}_{\tilde{r}}^m(\tau, \tau')] \\ &\quad - i \sum_{Z_1^{lr}, m_1} \mathcal{D}(t; Z^{lr}, m; Z_1^{lr}, m_1) [\tilde{h}_{Z^{lr},I}^m(\tau), [\tilde{h}_{Z_1^{lr},I}^{m_1}(\tau'), \mathcal{S}(\tau')BS^\dagger(\tau')]], \end{aligned} \quad (\text{S57})$$

where we define

$$\tilde{H}_{\Lambda,I}^{Z^{lr},m}(t, \tau') := \sum_{Z_1^{lr}} \sum_{m_1=0}^{\infty} \mathcal{D}(t; Z^{lr}, m; Z_1^{lr}, m_1) \tilde{h}_{Z_1^{lr},I}^{m_1}(\tau'). \quad (\text{S58})$$

Applying again the theorem in [3] yields

$$\begin{aligned} \|\tilde{G}_r^m(\tau, \tau)\| &\leq \|\tilde{G}_r^m(\tau, 0)\| + \int_0^\tau d\tau' \sum_{Z_1^{lr}, m_1} \mathcal{D}(t; Z^{lr}, m; Z_1^{lr}, m_1) \|\tilde{h}_{Z^{lr}, I}^m(\tau), [\tilde{h}_{Z_1^{lr}, I}^{m_1}(\tau'), \mathcal{S}(\tau') B \mathcal{S}^\dagger(\tau')]\| \\ &\leq \|\tilde{G}_r^m(\tau, 0)\| + \sum_{Z_1^{lr}, m_1} \mathcal{D}(t; Z^{lr}, m; Z_1^{lr}, m_1) 2 \|\tilde{h}_{Z^{lr}, I}^m\| \int_0^\tau d\tau' \|\tilde{h}_{Z_1^{lr}, I}^{m_1}(\tau'), \mathcal{S}(\tau') B \mathcal{S}^\dagger(\tau')\|, \end{aligned} \quad (\text{S59})$$

where $\|\tilde{h}_{Z^{lr}, I}^m(\tau)\| = \|\tilde{h}_{Z^{lr}, I}^m\|$ is time independent as per (S27), or otherwise it can be replaced by the corresponding time-independent bound as per (S31) and (S32). Clearly, Eq. (S59) comprises the desired relation for initiating all the remaining iterations.

Armed with these preparations, one can now derive the generalized HK series in the interaction picture by repeatedly inserting Eq. (S59) into Eq. (S52). This iterative procedure yields the following,

$$\begin{aligned} \|[A_I^\ell(t), \mathcal{S}(t) B \mathcal{S}^\dagger(t)]\| &\leq \|[A_I^\ell(t), B]\| + 2\|A_I^\ell(t)\| \sum_{Z_0^{lr}, m_0} \mathcal{D}_i(t; Z_0^{lr}, m_0) 2 \|\tilde{h}_{Z_0^{lr}, I}^{m_0}\| \|\mathcal{D}_f(t; Z_0^{lr}, m_0)\| \|B\| \int_0^t d\tau_0 \\ &+ 2\|A_I^\ell(t)\| \sum_{Z_0^{lr}, m_0} \mathcal{D}_i(t; Z_0^{lr}, m_0) 2 \|\tilde{h}_{Z_0^{lr}, I}^{m_0}\| \sum_{Z_1^{lr}, m_1} \mathcal{D}(t; Z_0^{lr}, m_0; Z_1^{lr}, m_1) 2 \|\tilde{h}_{Z_1^{lr}, I}^{m_1}\| \\ &\times \|\mathcal{D}_f(t; Z_1^{lr}, m_1)\| \|B\| \int_0^t d\tau_0 \int_0^{\tau_0} d\tau_1 + 2\|A_I^\ell(t)\| \sum_{Z_0^{lr}, m_0} \mathcal{D}_i(t; Z_0^{lr}, m_0) 2 \|\tilde{h}_{Z_0^{lr}, I}^{m_0}\| \sum_{Z_1^{lr}, m_1} \mathcal{D}(t; Z_0^{lr}, m_0; Z_1^{lr}, m_1) 2 \|\tilde{h}_{Z_1^{lr}, I}^{m_1}\| \\ &\times \sum_{Z_2^{lr}, m_2} \mathcal{D}(t; Z_1^{lr}, m_1; Z_2^{lr}, m_2) 2 \|\tilde{h}_{Z_2^{lr}, I}^{m_2}\| \|\mathcal{D}_f(t; Z_2^{lr}, m_2)\| \|B\| \int_0^t d\tau_0 \int_0^{\tau_0} d\tau_1 \int_0^{\tau_1} d\tau_2 + \dots, \end{aligned} \quad (\text{S60})$$

where similar to Eq. (S49), symbolically

$$\mathcal{D}_f(t; Z^{lr}, m) = \begin{cases} 1 & \text{if } \mathbb{B}[\tilde{h}_{Z^{lr}, I}^m(t)] \cap \mathbb{B}[B_I(t)] \neq \emptyset, \\ 0 & \text{otherwise.} \end{cases} \quad (\text{S61})$$

S5. LIEB-ROBINSON BOUND FROM THE DISCRETE CONVOLUTION

The nested structure of Eq. (S60) might be exploited to invoke the discrete convolution in reducing the infinite HK series to a closed form of the LR bound [2]. The basic strategy is to conceive a device in the discrete convolution to take advantage of the compromise between the exponential and the power-law decays as reflected by

$$\|\tilde{h}_{Z^{lr}, I}^m\| \leq \frac{c \cdot e^{-m}}{[1 + \text{diam}(Z^{lr})]^\eta}, \quad (\text{S62})$$

where Eqs. (S31), (S32), and (S9) have been used and the constant c properly encapsulates all the relevant parameters to ensure the validity of (S62) for any Z^{lr}, m .

Next, take a fixed Z_0^{lr} for example, one shall always be able to find a way to divide and assign a realization of L_0 and R_0 that satisfies $L_0 \cup R_0 = Z_0^{lr}$ and simultaneously fulfills the definitions of the nearby two D -functions that involve Z_0^{lr} . Since eventually L_0 and R_0 will be treated as two independent Z_0^{lr} , this step might lead to looser bound but should not cause any violation of the inequality. L_0 and R_0 can have overlaps. Now assume the existence of such a division, Eq. (S60) can then be rewritten as follows,

$$\begin{aligned} &\|[A_I^\ell(t), \mathcal{S}(t) B \mathcal{S}^\dagger(t)]\| \\ &\leq \|[A_I^\ell(t), B]\| + 2\|A_I^\ell(t)\| \sum_{L_0, R_0} \sum_{m_{0L}, m_{0R}} \mathcal{D}_i(t; L_0, m_{0L}) \times \frac{2c \cdot e^{-\frac{m_{0L} + m_{0R}}{2}}}{[1 + \text{dmax}(L_0, R_0)]^\eta} \|\mathcal{D}_f(t; R_0, m_{0R})\| \|B\| \int_0^t d\tau_0 \\ &+ 2\|A_I^\ell(t)\| \sum_{L_0, R_0} \sum_{m_{0L}, m_{0R}} \mathcal{D}_i(t; L_0, m_{0L}) \frac{2c \cdot e^{-\frac{m_{0L} + m_{0R}}{2}}}{[1 + \text{dmax}(L_0, R_0)]^\eta} \times \sum_{L_1, R_1} \sum_{m_{1L}, m_{1R}} \mathcal{D}(t; R_0, m_{0R}; L_1, m_{1L}) \end{aligned}$$

$$\begin{aligned}
& \times \frac{2c \cdot e^{-\frac{m_{1L}+m_{1R}}{2}}}{[1 + \text{dmax}(L_1, R_1)]^\eta} \mathcal{D}_f(t; R_1, m_{1R}) \|B\| \int_0^t d\tau_0 \int_0^{\tau_0} d\tau_1 \\
& + 2 \|A_I^\ell(t)\| \sum_{L_0, R_0} \sum_{m_{0L}, m_{0R}} \mathcal{D}_i(t; L_0, m_{0L}) \frac{2c \cdot e^{-\frac{m_{0L}+m_{0R}}{2}}}{[1 + \text{dmax}(L_0, R_0)]^\eta} \times \sum_{L_1, R_1} \sum_{m_{1L}, m_{1R}} \mathcal{D}(t; R_0, m_{0R}; L_1, m_{1L}) \\
& \times \frac{2c \cdot e^{-\frac{m_{1L}+m_{1R}}{2}}}{[1 + \text{dmax}(L_1, R_1)]^\eta} \sum_{L_2, R_2} \sum_{m_{2L}, m_{2R}} \mathcal{D}(t; R_1, m_{1R}; L_2, m_{2L}) \\
& \times \frac{2c \cdot e^{-\frac{m_{2L}+m_{2R}}{2}}}{[1 + \text{dmax}(L_2, R_2)]^\eta} \mathcal{D}_f(t; R_2, m_{2R}) \|B\| \int_0^t d\tau_0 \int_0^{\tau_0} d\tau_1 \int_0^{\tau_1} d\tau_2 + \dots, \tag{S63}
\end{aligned}$$

where in the final step, the summations have been relaxed to the independent subsets of L_i and R_i , whose maximal distance is denoted by $\text{dmax}(L_i, R_i)$. Analogous extensions also apply to the summations of the integer exponents.

Following Ref. [2], we perform the summation over the integer exponents first. Take the first term for example. If $\text{dmin}(R_0, L_1) \leq 2R(t)$, then

$$\sum_{m_{0R}=0}^{\infty} \sum_{m_{1L}=0}^{\infty} e^{-\frac{m_{0R}}{2}} \cdot \mathcal{D}(t; R_0, m_{0R}; L_1, m_{1L}) \cdot e^{-\frac{m_{1L}}{2}} = \sum_{m_{0R}=0}^{\infty} \sum_{m_{1L}=0}^{\infty} e^{-\frac{m_{0R}}{2}} \cdot e^{-\frac{m_{1L}}{2}} = \left(\frac{\sqrt{e}}{\sqrt{e}-1} \right)^2 = \delta^2. \tag{S64}$$

If instead $\text{dmin}(R_0, L_1) > 2R(t)$, then

$$\begin{aligned}
& \sum_{m_{0R}=0}^{\infty} \sum_{m_{1L}=0}^{\infty} e^{-\frac{m_{0R}}{2}} \cdot \mathcal{D}(t; R_0, m_{0R}; L_1, m_{1L}) \cdot e^{-\frac{m_{1L}}{2}} \\
& = \sum_{m_{0R}=\lceil \frac{\text{dmin}(R_0, L_1) - 2R(t)}{2\chi} \rceil}^{\infty} e^{-\frac{m_{0R}}{2}} \cdot \sum_{m_{1L}=0}^{\infty} e^{-\frac{m_{1L}}{2}} \leq \delta^2 e^{-[\text{dmin}(R_0, L_1) - 2R(t)]/4\chi}. \tag{S65}
\end{aligned}$$

In general,

$$\begin{aligned}
& \sum_{m_{iR}=0}^{\infty} \sum_{m_{i+1,L}=0}^{\infty} e^{-\frac{m_{iR}}{2}} \cdot \mathcal{D}(t; R_i, m_{iR}; L_{i+1}, m_{i+1,L}) \cdot e^{-\frac{m_{i+1,L}}{2}} \\
& = \mathcal{K}(t; R_i; L_{i+1}) = \begin{cases} \delta^2 & \text{if } \text{dmin}(R_i, L_{i+1}) \leq 2R(t), \\ \delta^2 e^{-[\text{dmin}(R_i, L_{i+1}) - 2R(t)]/4\chi} & \text{if } \text{dmin}(R_i, L_{i+1}) > 2R(t). \end{cases} \tag{S66}
\end{aligned}$$

According to this result, Eq. (S63) simplifies to

$$\begin{aligned}
& \sum_{\ell=0}^{\infty} \|[A_I^\ell(t), \mathcal{S}(t)BS^\dagger(t)]\| \leq \sum_{\ell=0}^{\infty} \|[A_I^\ell(t), B]\| + 2c_A \sum_{L_0, R_0} \mathcal{K}_i(t; L_0) \frac{2c}{[1 + \text{dmax}(L_0, R_0)]^\eta} \mathcal{K}_f(t; R_0) \|B\| \int_0^t d\tau_0 \\
& + 2c_A \sum_{L_0, R_0} \mathcal{K}_i(t; L_0) \frac{2c}{[1 + \text{dmax}(L_0, R_0)]^\eta} \sum_{L_1, R_1} \mathcal{K}(t; R_0; L_1) \times \frac{2c}{[1 + \text{dmax}(L_1, R_1)]^\eta} \mathcal{K}_f(t; R_1) \|B\| \int_0^t d\tau_0 \int_0^{\tau_0} d\tau_1 \\
& + 2c_A \sum_{L_0, R_0} \mathcal{K}_i(t; L_0) \frac{2c}{[1 + \text{dmax}(L_0, R_0)]^\eta} \sum_{L_1, R_1} \mathcal{K}(t; R_0; L_1) \frac{2c}{[1 + \text{dmax}(L_1, R_1)]^\eta} \\
& \times \sum_{L_2, R_2} \mathcal{K}(t; R_1; L_2) \frac{2c}{[1 + \text{dmax}(L_2, R_2)]^\eta} \mathcal{K}_f(t; R_2) \|B\| \int_0^t d\tau_0 \int_0^{\tau_0} d\tau_1 \int_0^{\tau_1} d\tau_2 + \dots, \tag{S67}
\end{aligned}$$

where the summation of the index ℓ has been first extended and then performed over the initial and final configurations and the constant c_A is defined by

$$c_A = \|A\| \|X\| p_0^{-1} s'(1+e). \tag{S68}$$

To make further progress, three key features of the constituent functions in (S67) need to be explored. First, it can be noticed from (S66) that in the region of short distance, function \mathcal{K} exhibits a flat plateau. Second, once beyond the dynamical length scale, \mathcal{K} decays exponentially. Third, the connecting function between the neighbouring \mathcal{K} functions decays in contrast as a power law of the separation as is inherited from Eq. (S62). Therefore, the observations that (1) function \mathcal{K} possesses a two-stage structure and (2) the hybridization of the exponential versus the power-law decaying functions play a vital role in the discrete convolution of the HK series.

We now proceed in three successive steps to obtain or better estimate the LR bound.

(1) Qualitatively, it is not hard to estimate the convolution of an exponentially decaying function with a power law, therefore

$$\begin{aligned} & \sum_{L_i} \mathcal{K}(t; R_{i-1}; L_i) \frac{1}{[1 + \text{dmax}(L_i, R_i)]^\eta} \\ & \leq \mathcal{F}(t; R_{i-1}; R_i) \approx \begin{cases} \lambda_\chi & \text{if } \text{dmin}(R_{i-1}, R_i) < wR(t), \\ \lambda_\chi \frac{[wR(t)]^\eta}{[1 + \text{dmin}(R_{i-1}, R_i)]^\eta} & \text{if } \text{dmin}(R_{i-1}, R_i) \geq wR(t). \end{cases} \end{aligned} \quad (\text{S69})$$

This result is based on several observations [2]. First, for those $\text{dmin}(R_{i-1}, R_i) < wR(t)$ where w is an adjust coefficient of order 1, function \mathcal{K} can be simply replaced by its maximum value δ^2 , then a dimensional analysis leads to the rough estimate that,

$$\sum_L \frac{1}{[1 + \text{dmax}(L, R)]^\eta} \lesssim \lambda \chi^{D-\eta}, \quad (\text{S70})$$

where λ is of order 1 and D is the spatial dimension. Thus,

$$\lambda_\chi := \lambda \delta^2 \chi^{D-\eta}. \quad (\text{S71})$$

Second, when $\text{dmin}(R_{i-1}, R_i) \geq wR(t)$, it is easy to understand that the major contributions of the summation shall come from those L_i 's that are closer to R_{i-1} so that the exponential suppression in \mathcal{K} can be compensated to some degree and the resulting convolution should then be approximated by an overall power law at long distance between R_{i-1} and R_i . Third, the continuity condition of \mathcal{F} at $\text{dmin}(R_{i-1}, R_i) \approx wR(t)$ finally sets the various forms of the coefficients. Be aware that the two-stage structure of function \mathcal{F} is a direct reflection of the two-stage structure of function \mathcal{K} . Accordingly, Eq. (S67) reduces to

$$\begin{aligned} & \sum_{\ell=0}^{\infty} \|[A_I^\ell(t), \mathcal{S}(t)B\mathcal{S}^\dagger(t)]\| \leq \sum_{\ell=0}^{\infty} \|[A_I^\ell(t), B]\| + 2c_A \sum_{R_0} 2c\mathcal{F}_i(t; R_0)\mathcal{K}_f(t; R_0)\|B\| \int_0^t d\tau_0 \\ & + 2c_A \sum_{R_0} 2c\mathcal{F}_i(t; R_0) \sum_{R_1} 2c\mathcal{F}(t; R_0; R_1)\mathcal{K}_f(t; R_1)\|B\| \int_0^t d\tau_0 \int_0^{\tau_0} d\tau_1 \\ & + 2c_A \sum_{R_0} 2c\mathcal{F}_i(t; R_0) \sum_{R_1} 2c\mathcal{F}(t; R_0; R_1) \times \sum_{R_2} 2c\mathcal{F}(t; R_1; R_2)\mathcal{K}_f(t; R_2)\|B\| \int_0^t d\tau_0 \int_0^{\tau_0} d\tau_1 \int_0^{\tau_1} d\tau_2 + \dots \end{aligned} \quad (\text{S72})$$

(2) The treatment of the discrete convolution of the \mathcal{F} functions relies on the cousin of the reproducing condition (S10), which basically states that

$$\sum_{R_i} \tilde{\mathcal{F}}(t; R_{i-1}; R_i) \tilde{\mathcal{F}}(t; R_i; R_{i+1}) \leq g[R(t)]^D \tilde{\mathcal{F}}(t; R_{i-1}; R_{i+1}), \quad (\text{S73})$$

where to keep the dimension correct, we redefine

$$\tilde{\mathcal{F}}(t; R_i; R_j) := \frac{1}{\lambda_\chi} \mathcal{F}(t; R_i; R_j). \quad (\text{S74})$$

(3) Finally, by noticing that generically power-law functions $\tilde{\mathcal{F}}$ decay more slowly than the exponential functions \mathcal{K} , one might be able to perform the following replacement,

$$\mathcal{K}_f(t; R) \implies \tilde{\mathcal{F}}_f(t; R). \quad (\text{S75})$$

Combine all these simplifications and do the integrals of times, one can readily obtain from Eq. (S72) the following,

$$\begin{aligned}
\sum_{\ell=0}^{\infty} \|[A_I^\ell(t), \mathcal{S}(t)B\mathcal{S}^\dagger(t)]\| &\leq \sum_{\ell=0}^{\infty} \|[A_I^\ell(t), B]\| + 2c_A\|B\| \cdot \frac{2c\lambda_\chi g[R(t)]^D}{\{\text{dist}(X, Y)/[wR(t)]\}^\eta} \cdot t \\
&+ 2c_A\|B\| \cdot \frac{\{2c\lambda_\chi g[R(t)]^D\}^2}{\{\text{dist}(X, Y)/[wR(t)]\}^\eta} \cdot \left(\frac{1}{2}t^2\right) \\
&+ 2c_A\|B\| \cdot \frac{\{2c\lambda_\chi g[R(t)]^D\}^3}{\{\text{dist}(X, Y)/[wR(t)]\}^\eta} \cdot \left(\frac{1}{3!}t^3\right) + \dots \\
&\leq \sum_{\ell=0}^{\infty} \|[A_I^\ell(t), B]\| + 2c_A\|B\|w^{-\eta} \cdot \frac{\exp\{2c\lambda_\chi g[R(t)]^D \cdot t\}}{[\text{dist}(X, Y)/R(t)]^\eta}. \tag{S76}
\end{aligned}$$

Next, the overall short-range contribution can be derived as follows.

$$\sum_{\ell=0}^{\infty} \|[A_I^\ell(t), B]\| \approx \sum_{\ell=\lceil \frac{r}{\chi} - vt \rceil}^{\infty} \|[A_I^\ell(t), B]\| \leq \sum_{\ell=\lceil \frac{r}{\chi} - vt \rceil}^{\infty} 2\|[A_I^\ell(t), B]\| \leq \sum_{\ell=\lceil \frac{r}{\chi} - vt \rceil}^{\infty} 4c_A\|B\|e^{-\ell} = 4c_A\|B\|\frac{e}{e-1}e^{vt-r/\chi}, \tag{S77}$$

where we have assumed that the sizes of the supports of operators A, B are negligibly small as compared to their separation $r := \text{dist}(X, Y)$ so that the involved commutators are nonzero only if

$$\ell \geq \frac{r}{\chi(0)} - \frac{\chi(t)vt}{\chi(0)} \gtrsim \frac{r}{\chi(t)} - vt. \tag{S78}$$

Here, we have also exclusively focused on the spacetime regimes that are close to the lightcone front. Hence, we finally obtain the LR bound through the interaction-picture formulation of a generic k -body nonlocal interacting Hamiltonian with power-law decaying strengths,

$$\begin{aligned}
\|[A_H(t), B]\| &\leq \sum_{\ell=0}^{\infty} \|[A_I^\ell(t), \mathcal{S}(t)B\mathcal{S}^\dagger(t)]\| \\
&\leq 4c_A\|B\|\frac{e}{e-1}e^{vt-\text{dist}(X, Y)/\chi(t)} + 2c_A\|B\|w^{-\eta} \cdot \frac{\exp\{2c\lambda_\chi g[R(t)]^D \cdot t\}}{[\text{dist}(X, Y)/R(t)]^\eta} \\
&= 2\|A\|\|X\|\|B\|p_0^{-1}s'(1+e) \left\{ \frac{2e}{e-1}e^{vt-\text{dist}(X, Y)/\chi(t)} + w^{-\eta} \cdot \frac{\exp\{2c\lambda_\chi g[R(t)]^D \cdot t\}}{[\text{dist}(X, Y)/R(t)]^\eta} \right\}. \tag{S79}
\end{aligned}$$

Up to some prefactors, the refined LR bound (S79) resembles that obtained by Ref. [2] and thus shares the same form of the standard LR bound in long-range power-law systems first derived by Hastings and Koma [4]. The essential improvement resides in the renormalization of the various contents dressed by the introduced dynamical length scale, which somehow can be anticipated from scratch. Be cautious, rather than directly working with the bare lattice Hamiltonian as was done in Refs. [2, 4], we have reformulated a modified Hastings-Koma series using the integral-of-motion representation, which is suitable in the context of MBL.

-
- [1] S. Bravyi, M. B. Hastings, and F. Verstraete, Lieb-Robinson Bounds and the Generation of Correlations and Topological Quantum Order, *Phys. Rev. Lett.* **97**, 050401 (2006).
[2] M. Foss-Feig, Z.-X. Gong, C. W. Clark, and A. V. Gorshkov, Nearly Linear Light Cones in Long-Range Interacting Quantum Systems, *Phys. Rev. Lett.* **114**, 157201 (2015).
[3] B. Nachtergaele, Y. Ogata, and R. Sims, Propagation of Correlations in Quantum Lattice Systems, *J. Stat. Phys.* **124**, 1 (2006).
[4] M. B. Hastings and T. Koma, Spectral Gap and Exponential Decay of Correlations, *Commun. Math. Phys.* **265**, 781 (2006).